EQUILIBRIUM AND DYNAMICS OF SURFACTANT ADSORPTION MONOLAYERS AND THIN LIQUID FILMS

by

Krassimir D. Danov, Peter A. Kralchevsky and Ivan B. Ivanov
Faculty of Chemistry, University of Sofia, Sofia, BULGARIA

TABLE OF CONTENTS

Part 1

I. INTRODUCTION

The interactions across a thin film, called the *surface forces*, to a great extent are determined by the surfactant adsorption at the film surfaces. From a physical viewpoint, a liquid film formed between two phases is termed "thin" when the interaction of the phases across the film is not negligible. Thin films appear between the bubbles in foams, between the droplets in emulsions, as well as between the particles in suspensions. Furthermore, the properties of the thin liquid film determine the stability of various colloids.

There are three scenarios for the behavior of two colliding particles in a dispersion (for example, emulsion) depending on the properties of the films (Fig. 1). (i) When the film formed upon particle collision is stable, flocks of attached particles can appear. (ii) When the attractive interaction across the film is predominant, the film is unstable and ruptures; this leads to coalescence of the drops in emulsions or of the bubbles in foams. (iii) If the repulsive forces are predominant, the two colliding particles will rebound and the colloidal dispersion will be stable. In some cases, by varying the electrolyte concentration or pH, it is possible to increase the repulsion between the particles in a flocculated dispersion and to cause the inverse process of peptisation [1].
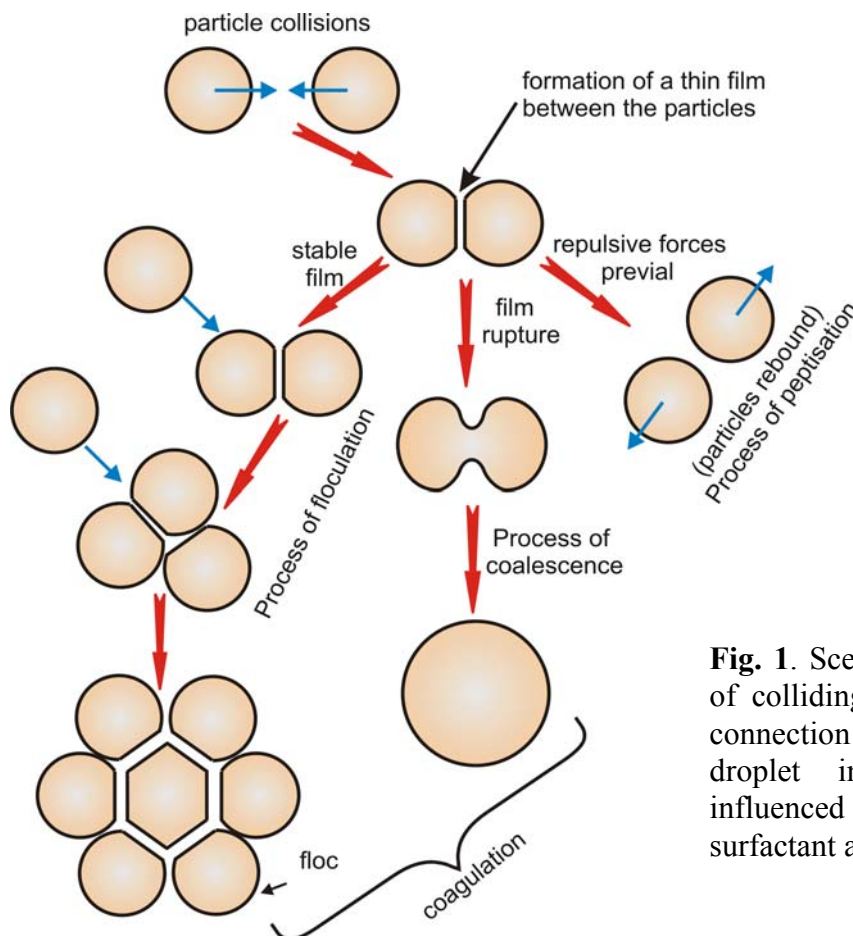
Fig. 1. Scenarios for the behavior of colliding emulsion droplets in connection with the droplet-droplet interaction, which is influenced by the properties of the surfactant adsorption monolayers.

1

The gap between two particles, like those depicted in Figure 1, can be considered as a liquid film of uneven thickness. The calculation of the particle-particle interaction energy can be reduced to the simpler calculation of the interaction across a plane-parallel film by using the Derjaguin formula, see Eq. (182) below. This is the reason why in this review we will pay much attention to the plane parallel films.

As already mentioned, the surfactants are used to stabilize the liquid films in foams, emulsions, on solid surfaces, etc. Below we first consider the equilibrium and kinetic properties of surfactant adsorption monolayers. Various two-dimensional *equations of state* are discussed. The *kinetics* of surfactant adsorption is described in the cases of *diffusion* and *barrier* control. Special attention is paid to the process of adsorption from *ionic* surfactant solutions. Theoretical models of the adsorption from *micellar* surfactant solutions are also presented. The *rheological* properties of the surfactant adsorption monolayers, such as dilatational and shear surface viscosity, and surface elasticity are introduced. The specificity of the proteins as high molecular weight surfactants is also discussed.

Next we consider the *flexural properties* of surfactant adsorption monolayers, which are important for the formation of small droplets, micelles and vesicles in the fluid dispersions. The contributions of various interactions (van der Waals, electrostatic, steric) into the interfacial bending moment and the curvature elastic moduli are described. The effect of interfacial bending on the interactions between deformable emulsion droplets is discussed.

Having reviewed the properties of single adsorption monolayers, we proceed with the couples of interacting monolayers: the *thin liquid films*. First we present the thermodynamics of thin films, and then we describe the molecular theory of the surface forces acting in the thin films. We do not restrict ourselves to the conventional *DLVO forces* [2,3], but consider also the variety of the more recently discovered *non-DLVO* surface forces [4]. The importance of the micelle-micelle interaction for the *mechanism of micelle growth* is also discussed.

In addition to the surface forces, *hydrodynamic forces* play an important role for the interactions in the real liquid films and colloidal dispersions. The hydrodynamic force is due to the viscous friction accompanying the expulsion of the liquid from the gap between two particles. When the particles are fluid (drops, bubbles) the fluidity of their surfaces (determined by the properties of the surfactant adsorption monolayers) can significantly affect the magnitude of the hydrodynamic force [5]. We consider the effect of the *surface elasticity, surface diffusion* and *surface viscosity* on the hydrodynamic force. All these effects are related to dilatational or shear deformations in the surfactant adsorption monolayer coupled

with the fluid fluxes in the bulk. Another effect of practical importance for emulsion preparation is the influence of diffusion transfer of surfactant *across* the film surfaces on the stability of the films. This effect is typical for emulsion systems, for which the surfactant is soluble in both the aqueous and the oil phase, but is initially put in one of the phases. When the surfactant is initially dissolved in the continuous phase, a phenomenon called *cyclic dimpling* is caused by the diffusion flux. In the opposite case, when the surfactant is initially dissolved in the drops, the diffusion brings about an *osmotic swelling* of the film. It is interesting to note that in both cases the diffusion of surfactant across the interfaces leads to stabilization of the liquid films and the emulsions.

Finally we consider the hydrodynamic theory of thin liquid film rupture. The stability of the liquid films to a great extent is ensured by the property of the adsorbed surfactant to damp the thermally excited fluctuation capillary waves representing peristaltic variations in the film thickness [6]. In addition to the theory of stability of *free* foam and emulsion films, we consider also the drainage and stability of *wetting* films, which find application in various coating technologies [7].

II. THERMODYNAMICS OF ADSORPTION FROM SURFACTANT SOLUTIONS

The fluid dispersions (emulsions, foams) are stabilized by adsorption layers of amphiphile molecules. These can be ionic and nonionic surfactants, lipids, proteins, etc. All of them have the property to lower the value of the surface (or interfacial) tension, σ, in accordance with the Gibbs adsorption equation [8-10],

$$\mathrm{d}\sigma = -kT\sum_i \Gamma_i \, \mathrm{d}\ln c_i \tag{1}$$

where k is the Boltzmann constant, T is temperature, c_i and Γ_i are respectively the bulk concentration and the surface concentration (adsorption) of the i-th component in the solution. The summation in Eq. (1) is carried out over all components. Usually an equimolecular dividing surface with respect to the solvent is introduced; the adsorption of the solvent is set zero by definition [8,9]. Then the summation is carried out over all other components. Γ_i itself is an excess surface concentration with respect to the bulk. Γ_i is positive for surfactants, which decrease σ in accordance with Eq.(1). On the opposite, Γ_i is negative for aqueous solutions of electrolytes, whose ions are repelled from the surface by the electrostatic image forces [9]; consequently, the addition of electrolytes increases the surface tension of water

[10]. When the interactions between the dissolved molecules/ions become important, c_i in Eq. (1) must be replaced with the respective activity.

A. Langmuir Adsorption Isotherm and its Generalizations

A relation between the bulk surfactant concentration, c, and the surfactant adsorption, Γ, is provided by the *Langmuir isotherm*,

$$\Gamma = \Gamma_\infty \frac{c}{B+c} \tag{2}$$

where Γ_∞ is the maximum possible adsorption at $c \to \infty$, and B is a constant, which can be related to the energy of adsorption per molecule [10-12]:

$$B = \frac{\Gamma_\infty}{\delta} \exp\left(\frac{\mu_0^s - \mu_0}{kT} \right) \tag{3}$$

Here δ is the thickness of the adsorption layer, μ_0^s and μ_0 are the standard chemical potentials of a surfactant molecule on the surface and in the bulk of solution; c and B are measured in cm^{-3}. In spite of the fact that Eq.(2) is originally derived for the special case of *localized* adsorption of non-interacting molecules, it can be successfully applied to various surfactants, including ionic ones [13-17]. The Langmuir isotherm can be generalized for multicomponent adsorption [18].

On integrating Eq. (1), along with Eq. (2), one obtains the Szyszkowski [19] equation relating σ and c,

$$\pi_s \equiv \sigma_0 - \sigma = kT\Gamma_\infty \ln(c / B + 1) \tag{4}$$

Here σ_0 is the surface tension of the pure solvent and π_s is called the surface pressure. Finally, by eliminating c between Eqs. (2) and (4) one derives the respective surface equation of state, often called the Frumkin [20] equation:

$$\pi_s = -kT\Gamma_\infty \ln\left(1 - \frac{\Gamma}{\Gamma_\infty}\right) \tag{5}$$

Equations (2)-(5) take into account neither the interaction between the adsorbed surfactant molecules, nor the electrostatic energy of the surfactant ion (in case of ionic surfactant). Borwankar and Wasan [21] generalized the Langmuir isotherm, Eq. (2), to account for the latter two effects:

$$\frac{\Gamma}{\Gamma_\infty - \Gamma} \exp\left(-A \frac{\Gamma}{\Gamma_\infty} \right) \exp\left(\frac{Ze\psi_s}{kT} \right) = c / B \tag{6}$$

where Z is the valence of the surfactant ion ($Z=0$ for a nonionic surfactant), e is the elementary charge, ψ_s is the surface electric potential (provided that the electric potential in the bulk of solution is zero), A is a constant accounting for the non-electrostatic interactions among the adsorbed amphiphiles. The combination of Eq. (6) with the general Gibbs equation (1) and with the Gouy-Chapman theory of the electric double layer [3] yields the following two-dimensional equation of state [21], generalizing Eq. (5):

$$\pi_S = -kT\Gamma_\infty \left[\ln\left(1 - \frac{\Gamma}{\Gamma_\infty}\right) + \frac{A}{2}\left(\frac{\Gamma}{\Gamma_\infty}\right)^2 \right] + \sqrt{\frac{8\varepsilon C(kT)^3}{\pi e^2}}\left(\cosh\frac{e\psi_S}{2kT} - 1\right) \tag{7}$$

where ε is the dielectric constant of the solution and the surface active ion, as well as the added electrolyte, is assumed monovalent; C denotes the total electrolyte concentration (surfactant + added salt) [21]. In the case of non-ionic surfactant one can use Eq. (7) after setting formally $\psi_s = 0$. Note that ψ_s in Eqs. (6) and (7) depends on Γ: the connection between surface charge and surface potential provided by the double layer theory [3],

$$\Gamma = \sqrt{\frac{8\varepsilon CkT}{\pi e^2}} \sinh\left|\frac{e\psi_s}{2kT}\right| \tag{8}$$

may be used.

There has been a discussion in the literature whether the non-ionic surfactants in solution do bear some charge because of the adsorption of ions (say OH⁻) on the ethylene-oxide chains. Recent precise electrophoretic measurements with air bubbles and oil droplets in pure water or non-ionic surfactant solutions reveal that the observed negative surface charge is an inherent property of the interface water-hydrophobic phase (air, oil), which can be attributed to the adsorption of hydroxyl ions at the interface [22]. The non-ionic surfactant molecules, themselves, are not charged, but they can reduce the surface charge by displacing the adsorbed OH⁻ from the interface; for details see Ref. [22] and the literature cited therein.

B. Van der Waals Type Adsorption Isotherms

Another type of adsorption isotherms are based on the two-dimensional *van der Waals* equation of state [23],

$$\left(\pi_S + \frac{\beta}{a^2}\right)(a - a_\infty) = kT \tag{9}$$

corresponding to the case of *non-localized* adsorption; here $a = 1/\Gamma$ is the area per molecule, $a_\infty = 1/\Gamma_\infty$ is the excluded area per molecule and β accounts for the interactions between the

adsorbed molecules. The statistical theory [23,24] relates the parameters a_∞ and β with the potential of interaction, $u(r)$, between two adsorbed surfactant molecules:

$$a_\infty = \pi \int_0^{r_c} \left[1 - \exp\left(-\frac{u(r)}{kT} \right) \right] r\,dr \approx \frac{\pi}{2} r_c^2 \qquad (10)$$

$$\beta = -\pi kT \int_{r_c}^{\infty} \left[1 - \exp\left(-\frac{u(r)}{kT} \right) \right] r\,dr \approx -\pi \int_{r_c}^{\infty} u(r)\, r\,dr \qquad (11)$$

where r_c is the intermolecular center-to-center distance at contact, i.e. $u(r) \to \infty$ for $r < r_c$. Eq. (10) and (11) explicitly shows that a_∞ and β account for the hard-core and long-range interactions, respectively. Combining Eqs. (9) and (1) one obtains the relation between c and a in the van der Waals approach:

$$\frac{a_\infty}{a - a_\infty} \exp\left(-\frac{2\beta}{akT} + \frac{a_\infty}{a - a_\infty} \right) = c/B \qquad (12)$$

where the constant B is given by Eq. (3).

Note that the integral in Eq. (11) is convergent only when $u(r)$ tends to zero faster than r^{-2} for $r \to \infty$, for example such is the case of dipole-dipole interaction. In the case of the slowly decaying Coulombic interaction between adsorbed surfactant *ions*, generalized versions of Eq. (9) and (12) can be derived

$$\pi_S = -\frac{\beta}{a^2} + \frac{kT}{a - a_\infty} + \sqrt{\frac{8\varepsilon C (kT)^3}{\pi e^2}} \left(\cosh\frac{e\psi_s}{2kT} - 1 \right) \qquad (13)$$

$$\frac{a_\infty}{a - a_\infty} \exp\left(-\frac{2\beta}{akT} + \frac{a_\infty}{a - a_\infty} + \frac{e\psi_s}{kT} \right) = c/B \qquad (14)$$

Eqs. (13) and (14) are counterparts of Eqs. (7) and (6), respectively. For $\beta = 0$ Eq. (13) reduces to the equation derived by Davies [25] and Hachisu [26]. In view of Eq. (.8) one finds that the last term in Eq. (13) decreases, when the total electrolyte concentration C increases at fixed area per molecule, a. This would lead to a decrease in π_S, if a were really constant. However, Eqs. (8) and (14) show that a decreases when C increases at fixed surfactant concentration c, which leads to an increase of π_S. The competition between these two opposite trends determines the dependence of π_S on the electrolyte concentration C. For sodium dodecylsulfate the second trend (the decrease of a) is predominant and π_S increases with the increase of C at fixed c.

Expanding in series for $a_\infty/a \ll 1$, from Eq. (9) one can derive

$$\frac{\pi_S a}{kT} = 1 + \left(1 - \frac{\beta}{kTa_\infty}\right)\frac{a_\infty}{a} + O\left(\frac{a_\infty^2}{a^2}\right) \tag{15}$$

Hence, for $a_\infty/a \ll 1$ the plot of $\pi_S a/(kT)$ vs. a_∞/a should be a straight line of intercept 1. However, in some cases an intercept close to 1/2 can be found: see Ref.[27]. This can be attributed to the formation of doublets of adsorbed molecules due to the component of their dipole moments oriented laterally to the interface. This effect can be observed with zwitterionic amphiphiles like some lipids [27]. A doublet represents a couple of adsorbed molecules with *antiparallel* orientations of their lateral dipole moments.

In addition, it should be noted that various semi-empirical surface equations of state can be used, see e.g. Ref. [28]. For example, Tajima et al. [29] proposed the following equation for sodium dodecylsulfate:

$$\left(\pi_S + 6.03\,C^{1/2} + \frac{0.43\,kT}{a}\right)\left(a - a_\infty\right) = kT \tag{16}$$

with $a_\infty = 38.4$ Å^2. Similar dependence of π_S on C can be deduced from Eqs. (8) and (13) for high value of the surface potential ψ_s.

Finally, we give the general definition of Gibbs elasticity [8]:

$$E_G = a\frac{\partial\sigma}{\partial a} = -\Gamma\frac{\partial\sigma}{\partial\Gamma} \tag{17}$$

E_G characterizes the increase of the surface tension with the quasistatic dilatation of the adsorption monolayer.

For the reader's convenience some of the most frequently used adsorption isotherms and surface equations of state (that of Henry, Langmuir, Freundlich, Volmer, Frumkin and van der Waals) [35,49-51] are summarized in Table 1; the respective expressions for $\partial\Gamma/\partial c$, and the Gibbs elasticity, E_G, stemming from the various isotherms are also given; Γ_F, B_F and m are characteristic parameters of the Freundlich adsorption isotherm.

Table 1. The most frequently used adsorption isotherms

	• **Adsorption isotherm**
Henry	$\Gamma / \Gamma_\infty = c / B$
Langmuir	$\Gamma / \Gamma_\infty = c / (B + c)$
Freundlich	$\Gamma / \Gamma_F = (c / B_F)^m$
Volmer	$c / B = \Gamma \exp[\Gamma / (\Gamma_\infty - \Gamma)] / (\Gamma_\infty - \Gamma)$
Frumkin	$c / B = \Gamma \exp(-2\beta\Gamma / kT) / (\Gamma_\infty - \Gamma)$
van der Waals	$c / B = \Gamma \exp[\Gamma / (\Gamma_\infty - \Gamma) - 2\beta\Gamma / kT] / (\Gamma_\infty - \Gamma)$
	• **Equation of state**
Henry	$\sigma = \sigma_0 - kT\Gamma$
Langmuir	$\sigma = \sigma_0 + kT\Gamma_\infty \ln(1 - \Gamma / \Gamma_\infty)$
Freundlich	$\sigma = \sigma_0 - kT\Gamma / m$
Volmer	$\sigma = \sigma_0 - kT\Gamma_\infty \Gamma / (\Gamma_\infty - \Gamma)$
Frumkin	$\sigma = \sigma_0 + kT\Gamma_\infty \ln(1 - \Gamma / \Gamma_\infty) + \beta\Gamma^2$
van der Waals	$\sigma = \sigma_0 - kT\Gamma_\infty \Gamma / (\Gamma_\infty - \Gamma) + \beta\Gamma^2$
	• $\partial\Gamma / \partial c$
Henry	Γ / c
Langmuir	$\Gamma_\infty B / (B + c)^2$
Freundlich	$m\Gamma / c$
Volmer	$\Gamma(1 - \Gamma / \Gamma_\infty)^2 / c$
Frumkin	$\dfrac{\Gamma}{c} \bigg/ \left(\dfrac{\Gamma_\infty}{\Gamma_\infty - \Gamma} - \dfrac{2\beta\Gamma}{kT} \right)$
van der Waals	$\dfrac{\Gamma}{c} \bigg/ \left[\dfrac{\Gamma_\infty^2}{(\Gamma_\infty - \Gamma)^2} - \dfrac{2\beta\Gamma}{kT} \right]$
	• $E_G = -\partial\sigma / \partial\ln\Gamma$
Henry	$kT\Gamma$
Langmuir	$kT\Gamma / (1 - \Gamma / \Gamma_\infty)$
Freundlich	$kT\Gamma / m$
Volmer	$kT\Gamma / (1 - \Gamma / \Gamma_\infty)^2$
Frumkin	$kT\Gamma \left(\dfrac{\Gamma_\infty}{\Gamma_\infty - \Gamma} - \dfrac{2\beta\Gamma}{kT} \right)$
van der Waals	$kT\Gamma \left[\dfrac{\Gamma_\infty^2}{(\Gamma_\infty - \Gamma)^2} - \dfrac{2\beta\Gamma}{kT} \right]$

III. KINETICS OF ADSORPTION FROM SURFACTANT SOLUTION

Not only the equilibrium surface tension, but also the kinetic properties of a surfactant adsorption monolayer play an important role in various phenomena related to the stability of foams and emulsions [5, 30], rising of bubbles and flotation [31]. Indeed, many processes are accompanied by disturbances (expansion, compression) of the adsorption monolayer or by formation of new surface of the solution. The surfactant solution has the property to damp the disturbances by diffusion of surfactant from the bulk to the interface, or vise versa. The main subject of the present Section III is the theory of adsorption and surface tension under such dynamic conditions.

Different experimental techniques have been developed for the measurement of dynamic surface tension. The most popular among them are the oscillating jet method [32], the inclined plate method [33], the maximum bubble pressure (MBP) method [34-39], the surface wave techniques [40-43], the oscillating bubble method [44-48], the drop weight techniques [14, 49-51], and the free falling film method [52, 53]. Detailed reviews on the experimental techniques can be found in the book by Dukhin *et al.* [31] and the paper by Franses *et al.* [54].

As mentioned earlier, below we focus our attention on the kinetics of surfactant adsorption. First we introduce the basic equations. Next we consider the two alternative cases of surfactant adsorption: under *diffusion* and *barrier* control. Special attention is paid to the adsorption of *ionic surfactants*, whose molecules are involved in long-range elecrtostatic interactions. Finally, we consider the adsorption from *micellar surfactant solutions*, which is accompanied by micelle diffusion, assembly or disintegration.

A. Basic equations

The basic equation describing the transport of the *i*-th solute in solution is the *mass-balance equation* (see Refs. 55-58)

$$\frac{\partial c_i}{\partial t} + \nabla \cdot (c_i \mathbf{v}) = \nabla \cdot \left(D_i \nabla c_i + D_i \frac{q_i c_i}{kT} \nabla \psi \right) + R_i, \quad i = 1, 2, ..., N; \tag{18}$$

where ∇ is the spatial gradient operator, t is the time, $\mathbf{v}$ is the mean mass velocity, q_i and D_i are the electric charge and the diffusion coefficient of the *i*-th solute and R_i is its rate of production in chemical reactions; ψ is the potential of the electric field; N denotes the total

number of the solutes; the meaning of c_i, k and T is the same as in Eq. (1). The term $\nabla \cdot (c_i \mathbf{v})$ in Eq. (18), called the *convective term*, accounts for the transport of component i by hydrodynamic fluxes; this term is essential for some methods of dynamic surface tension measurement accompanied by liquid flow, like the maximum bubble pressure method [14,35]. The terms with ∇c_i and $\nabla \psi$ take into account the contributions of the *diffusion* and *electric current* into the overall mass balance. Of course, the electric term is zero for the non-charged species. Usually the liquids are treated as incompressible fluids, i.e. $\nabla \cdot \mathbf{v} = 0$. Then the convective term in Eq. (18) can be simplified:

$$\nabla \cdot (c_i \mathbf{v}) = \mathbf{v} \cdot \nabla c_i \qquad (19)$$

Note that the diffusivity, D_i, and the kinematic viscosity of the liquid, ν, have the same physical dimension (cm^2/s). Their ratio $Sc = D_i /\nu$, called the Schmidt number, is usually small, of the order of 10^{-3}. The latter fact has the consequence that the diffusion boundary layer is much thinner than the hydrodynamic boundary layer in dynamic problems [59].

A two-dimensional analogue of Eq. (18), expressing the surface mass balance, holds at the interface:

$$\frac{\partial \Gamma_i}{\partial t} + \nabla_{\text{II}} \cdot \left(\Gamma_i \mathbf{v}_s \right) = \nabla_{\text{II}} \cdot \left(D_i^s \nabla_{\text{II}} \Gamma_i + D_i^s \frac{q_i \Gamma_i}{kT} \nabla_{\text{II}} \psi \right) + r_i - \mathbf{n} \cdot \langle \mathbf{J}_i \rangle, \quad i = 1, 2, \ldots, N_s; \qquad (20)$$

Here ∇_{II} is the surface gradient operator, N_s denotes the number of adsorbed components, Γ_i is the adsorption of component i, $\mathbf{v}_s$ is the surface velocity, D_i^s is the coefficient of surface diffusion, and r_k is the *rate of production* of component k by interfacial chemical reactions; $\mathbf{n}$ is the running unit normal to the surface, $\mathbf{J}_i$ is the subsurface value of the bulk electrodiffusion flux

$$\mathbf{J}_i \equiv -D_i \left(\nabla c_i + \frac{q_i c_i}{kT} \nabla \psi \right); \qquad (21)$$

the symbol $\langle \mathbf{J}_i \rangle$ denotes the difference between the values of $\mathbf{J}_i$ on the upper and lower side of the interface; the term with $\langle \mathbf{J}_i \rangle$ in Eq. (20) accounts for the exchange of component i between the adsorption layer and the two adjacent bulk phases.

Note that some of the components present at the interface may not be present in the bulk. An example are the insoluble surfactants. Another example represent components which appear and disappear only in specific interfacial chemical reactions (for example conformation of the adsorbed protein molecules from ball to long loop structures [60]).

In general, Eq. (20) serves as a boundary condition for the diffusion problem; it provides an expression for ∇c_i at the surface. In addition, boundary conditions for c_i can be used. These can be adsorption isotherms, like Eqs. (2), (6) or (14), relating subsurface concentration and adsorption. In the case of liquid-liquid interface one can use also a boundary condition expressing the equilibrium partitioning of a given solute between the two neighboring liquids [58]:

$$c_i(0+) = K_i c_i(0-) \qquad (i = 1, 2, ..., N) \tag{22}$$

Here K_i is the surface partition coefficient of component i; $c_i(0+)$ and $c_i(0-)$ denote the values of c_i on the two sides of the interface. At equilibrium Eq. (22) connects the bulk concentrations, whereas for dynamic processes (under diffusion control) Eq. (22) connects the subsurface concentrations only [58].

In general, the surfactant adsorption is a consequence of two stages: the first stage is the diffusion of surfactant from the bulk solution to the subsurface; the second stage is the transfer of the surfactant molecules from the subsurface to the surface. The following important cases of surfactant adsorption kinetics can be specified:

(i) *Diffusion-controlled* adsorption: the first stage (the surfactant diffusion) is much slower than the second stage and, consequently, determines the rate of adsorption. This case, which is very usual in practice, is considered theoretically in Subsection B below.

(ii) *Barrier-controlled* adsorption: the second stage is much slower than the diffusion because of the presence of some kinetic barrier, which slows down the transfer of the surfactant molecules from the subsurface to the adsorption monolayer. This barrier can be due to steric hindrance, electrostatic repulsion or conformational changes accompanying the adsorption of some molecules (usually polymers or proteins) - see Subsection C for details.

(iii) *Electrodiffusion-controlled* adsorption: this is the case of adsorption of ionic surfactants. Since the extent of the electric double layer is much larger than the size of the surfactant ions, the electrostatic interactions affect both the diffusion and the surfactant transfer from the subsurface to the surface. This case needs a special theoretical treatment, which is reviewed in Subsection D below.

(iv) *Adsorption from micellar solution:* in this case both surfactant monomers and micelles are involved in the diffusion process. Thus the micelles serve as carriers of surfactant from the bulk to the surface and vice versa. The reactions of micelle formation and decay should be necessarily taken into account, see Subsection E for details.

B. Adsorption under Diffusion Control

Let us consider the case of *diffusion-controlled adsorption* of electroneutral molecules at an interface, which is subjected to uniform expansion or compression. The interfacial expansion or compression is accompanied by hydrodynamic flux, which can be expressed by the equation of van Voorst Vader *et al.* [61]:

$$v_x = -x\dot{\alpha}(t) \tag{23}$$

where the *x*-axis is directed perpendicular to the solution surface inwards, v_x is the *x*-component of the velocity $\mathbf{v}$, $A(t)$ denotes the interfacial area and $\dot{\alpha}(t)$ is the rate of interfacial dilatation. Then, in view of Eqs. (19), (21) and (23), one can transform Eqs. (18) and (20) to read

$$\frac{\partial c_k}{\partial t} - x\dot{\alpha}\frac{\partial c_k}{\partial x} = \frac{\partial}{\partial x}\left(D_k\frac{\partial c_k}{\partial x}\right) \qquad (x > 0, \quad t > 0) \tag{24}$$

$$\frac{d\Gamma_k}{dt} + \dot{\alpha}\Gamma_k = D_k\frac{\partial c_k}{\partial x} \qquad (x = 0, t > 0) \tag{25}$$

To specify the initial conditions, let us assume that at the moment $t = 0$ the bulk concentration is equal to the equilibrium one, $c_{k,e}$, and that the initial adsorption of each component, $\Gamma_{k,0}$, is known.

B.1. Kinetics of adsorption at quiescent surface

If the interfacial expansion (compression) happens *only* at the initial moment and then the interface is quiescent (i.e. $\dot{\alpha} \equiv 0$ for $t > 0$), the relaxation of the surfactant adsorption is described by the expression of Ward and Tordai [62]:

$$\Gamma_k = 2\sqrt{\frac{D_k}{\pi}}\int_0^t\left[c_{k,e} - c_{k,s}(t - \tau)\right]d\sqrt{\tau} + \Gamma_{k,0} \qquad (k = 1, 2, \ldots, N) \tag{26}$$

which is a corollary of Eqs. (24) and (25); $c_{k,s}$ is the subsurface concentration and τ is a variable of integration. Eq. (26) coupled with a given adsorption isotherm, $\Gamma_k(c_{k,s})$, represents a Volterra integral system of equations, which, in general, has no analytical solution. In the case of one surfactant component a numerical procedure for solving the Eq. (26) with any adsorption isotherm is presented in Refs. [63-65]; expansions in power series for some of the most important isotherms are also available [66-68].

In the special case of single amphiphilic component and *small deviations* from equilibrium, the boundary problem can be linearized and Eq. (26) yields [69]

$$\frac{\Gamma_e - \Gamma(t)}{\Gamma_e - \Gamma(0)} = \frac{\sigma(t) - \sigma_e}{\sigma(0) - \sigma_e} = \frac{c_s(t) - c_e}{c_s(0) - c_e} = \exp\left(\frac{t}{t_r}\right) \mathrm{erfc}\left(\sqrt{\frac{t}{t_r}}\right) \quad , \quad t_r \equiv \frac{1}{D}\left(\frac{\partial \Gamma}{\partial c}\right)^2_{c=c_e} \quad , \quad (27)$$

where Γ_e is the equilibrium adsorption corresponding to bulk surfactant concentration c_e, c_s is the subsurface concentration; t_r is the characteristic relaxation time of adsorption, and erfc(x) is error function, see e.g Ref. [70]. (Theoretical approaches to the case of *large* deviations from equilibrium are described in section B.2 below.) The values of $\partial \Gamma / \partial c$ for some of the most frequently used adsorption isotherms (that of Henry, Langmuir, Freundlich, Volmer, Frumkin and van der Waals) are given in Table 1. Eq. (27) can be generalized for micellar solutions, see Eq. (70) below.

The generalizations of Eqs. (26) and (27) to the case of surfactant soluble in *two* adjacent liquid phases have been obtained by Miller [71]. It was demonstrated that the distribution coefficient, K_i, see Eq. (22), can be determined from experimental data for the dynamic interfacial tension. Since this coefficient is closely related to the HLB-value [72], such experiments would be useful to characterize the application of surfactants as emulsifiers.

The problem for the diffusion controlled adsorption of a *mixture* of surfactants at *small deviation* from equilibrium can be solved analytically by using the Laplace transform; the resulting long expressions can be found in Ref. 73. The results are compared with experimental data for different alkanoates at air-liquid interface [73]. Simple adsorption isotherms for mixtures of surfactants are reported in Refs. [31, 44]; surface equations of state applicable to mixtures of surfactant molecules of *different size* can be found in Refs. [27, 74].

When the initial deviation from equilibrium is *not* small, an exact general analytical expression for $\sigma(t)$ cannot be derived. However, explicit asymptotic expressions for long times ($t \to \infty$) and short times ($t \to 0$) of adsorption can be obtained, even for surfactant blends. The *long* time asymptotics of the subsurface concentration, $c_{i,s}$,

$$c_{i,e} - c_{i,s} = \left(\Gamma_{i,e} - \Gamma_{i,0}\right)\left(\frac{\pi}{D_i t}\right)^{1/2} + o(\frac{1}{\sqrt{t}}) \qquad \left(i = 1, 2, \ldots, N\right) , \qquad (28)$$

has been derived by Hansen [75], and further generalized in Refs. [31, 44, 73, 76, 77]. Here $\Gamma_{i,e}$ is the equilibrium adsorption corresponding to bulk concentration $c_{i,e}$. It is to be noted that many authors have reported Eq. (28) with a wrong factor 4 before D_i (see Ref. 76); however, the validity of Eq. (28) has been rigorously proved [78].

Using the Gibbs adsorption equation for a multicomponent solution (this is Eq. (1) with $c_i \equiv c_{i,s}$), one can derive the *long* time asymptotics of the surface tension

$$\sigma(t) - \sigma_e = \sum_{i=1}^{N} \frac{kT\Gamma_{i,e}\left(\Gamma_{i,e} - \Gamma_{i,0}\right)}{c_{i,e}} \left(\frac{\pi}{D_i t}\right)^{1/2} + o(\frac{1}{\sqrt{t}}) \tag{29}$$

where σ_e is the equilibrium surface tension. The assumption for independence on the various surfactant species, implicitly used to derive Eqs. (28) and (29), might be violated for large values of the adsorption. On the other hand, Eq. (29) is independent of the type of the adsorption isotherm, cf. Table 1.

The *short* time asymptotics of the adsorption has the following form [31, 44, 73, 76, 77]

$$\Gamma_i - \Gamma_{i,0} = \left(c_{i,e} - c_{i,0}\right)\left(\frac{4D_i t}{\pi}\right)^{1/2} + o\left(\sqrt{t}\right) \qquad (i = 1,2,\dots,N) \tag{30}$$

where $c_{i,0}$ is the initial subsurface concentration corresponding to the initial adsorption $\Gamma_{i,0}$. Then substituting Eq. (30) in the Gibbs adsorption equation one obtains the *short* time asymptotics of the surface tension reads

$$\sigma(t) - \sigma(0) = -\sum_{i=1}^{N} kT\left(c_{i,e} - c_{i,0}\right)\left(\frac{4D_i^* t}{\pi}\right)^{1/2} + o\left(\sqrt{t}\right) \tag{31}$$

where $\sigma(0)$ is the surface tension at the initial moment, and the mean diffusion coefficients are defined by expressions

$$D_k^* = D_k \left[\sum_{i=1}^{N} \Gamma_{i,0} \left(\frac{\partial \ln c_i}{\partial \Gamma_k}\right)_{c_i = c_{i,0}}\right]^2 \qquad (k = 1,2,\dots,N) \tag{32}$$

In the special case of single surfactant and initially clean surface, $\Gamma_0 = 0$, Eq. (29) and (31) reduce to

$$\sigma - \sigma_e \approx \frac{kT\Gamma_e^2}{c_e}\left(\frac{\pi}{Dt}\right)^{1/2} \quad , \qquad \sigma(0) - \sigma \approx kT c_e \left(\frac{4Dt}{\pi}\right)^{1/2} \tag{33}$$

Eqs. (28)-(33) refer to the limiting cases $t \to \infty$ and $t \to 0$, however no analytical expression is available for the intermediate times. Sometimes, empirical formulas are employed to process experimental data for the intermediate times. Rosen *et al.* [79-81] proposed the following empirical equation

$$\frac{\sigma_0 - \sigma_{me}}{\sigma - \sigma_{me}} = 1 + \left(\frac{t}{t^*}\right)^n \tag{34}$$

where σ_{me} is a "mesoequilibrium" surface tension of the solution (for which σ shows only small changes with time), σ_0 is the equilibrium surface tension of the pure solvent; t^* and n

are adjustable parameters, which have been determined for a large amount of experimental data [79-81].

A general (though approximate) theoretical approach to the calculation of $\Gamma(t)$ and $\sigma(t)$ for any magnitude of the surface deformation is presented below, see Eqs. (41)-(42).

B.2. Kinetics of adsorption at expanding surface ($\dot{\alpha} \neq 0$)

In many experimental techniques used for dynamic surface tension measurements (such as the MBP method and the drop volume method [14, 76, 82]) the surface expands gradually with time. In such a case the convective terms in Eqs. (24) and (25) cannot be neglected. Nevertheless, it can be demonstrated that with the help of the new independent variables,

$$z = xs(t) \quad \text{and} \quad \theta = \int_0^t s^2(\tau)d\tau, \quad \text{where} \quad s \equiv \frac{A(t)}{A(0)} \quad , \tag{35}$$

Eqs. (24) and (25) acquire the form of diffusion equations with constant coefficients:

$$\frac{\partial c_i}{\partial \theta} = D_i \frac{\partial^2 c_i}{\partial z^2}, \qquad \frac{d(s\Gamma_i)}{d\theta} = D_i \frac{\partial c_i}{\partial z}\bigg|_{z=0} \tag{36}$$

Eqs. (36) lead to a result, which is similar to the Ward-Tordai expression, Eq. (26):

$$s\Gamma_i = 2\sqrt{\frac{D_i}{\pi}} \int_0^\theta \left[c_{i,e} - c_{i,s}(\theta - \tau) \right] d\sqrt{\tau} + \Gamma_{i,0} \qquad (i = 1, 2, ..., N) \tag{37}$$

The solution of Eq. (37) for *small* surface deformations is obtained in Refs. [83, 84] and it is applied there for the interpretation of experimental data at known expansion rate, $s(t)$. However, there is no analytical solution of Eq. (37) for the case of *large* surface deformations. Nevertheless, analytical expressions for the long and short time asymptotics of Eq. (37) can be derived. In the case of single component and initially clean surface, $\Gamma(0) = 0$, the following short time asymptotics stems from Eq. (37):

$$\Gamma = c_e \left[\frac{4Dt}{\pi(2\alpha_d + 1)} \right]^{1/2} \quad , \qquad \alpha_d = \lim_{t \to 0}(t\dot{\alpha}) \tag{38}$$

Substituting $\alpha_d = 2/3$ in Eq. (38), one obtains the Joos formula, which has been applied to interpret experimental data from the MBP method [14, 76, 82].

A way to simplify the adsorption problem in the case of *large* surface deformations has been proposed by Kralchevsky *et al.* [35]. In so far as one is interested in the time dependence of the surface properties, $\Gamma(t)$ and $\sigma(t)$, one can use an appropriate *model*

expression, $c^*(x,t)$, for the surfactant concentration profile. Thus one avoids the time consuming numerical integration of the *partial* differential equation of surfactant diffusion. The function $c^*(x,t)$ must satisfy the following integral condition for equivalence between the *real* and *model* concentration profiles [35]:

$$\int_0^\infty \left[1 - \frac{c(x,t)}{c_e}\right] dx = \int_0^\infty \left[1 - \frac{c^*(x,t)}{c_e}\right] dx \equiv l(t) \tag{39}$$

Similarly to the von Karman boundary layer theory [85], the following model profile can be used [35]:

$$c^*(x,t) = c_s(t) + \left[c_e - c_s(t)\right]\sin\left(\frac{\pi x}{2\delta}\right) \quad \text{for } x \le \delta;$$

$$c^*(x,t) = c_e \qquad\qquad\qquad\qquad \text{for } x \ge \delta \tag{40}$$

where $c_s(t)$ is the subsurface concentration, see Fig. 2. Note the smooth matching of the sine with the line $c = c_e = $ const at the point $x = \delta$. The parameter δ is determined by substituting Eq. (40) into Eq. (39). Finally, this approach leads to the following equation for $\Gamma(t)$ [35]:

$$\Gamma(t) = c_e l(t) + [\Gamma(0) - c_e l(0)] / s(t) \tag{41}$$

where $s(t)$ is a known function defined by Eq.(35) and $l(t)$ satisfies the *ordinary* differential equation [35]

$$\frac{dl}{dt} + \dot{\alpha}(t)l(t) = \left(\frac{\pi}{2} - 1\right)\left[1 - \frac{c_s(t)}{c_e}\right]^2 \frac{D}{l(t)} \tag{42}$$

Eqs. (41), (42) and the adsorption isotherm, $c_s = c_s(\Gamma)$, (the latter can be any isotherm like those in Table 1) form a set of three equations for determining the three unknown functions $\Gamma(t)$, $l(t)$ and $c_s(t)$. The problem can be solved by numerical integration of Eq. (42). The initial condition depends on the specific problem; for example, if only the surface, but not the solution, is disturbed in the initial moment, i.e. $c(x,0) = c_e$ for $x > 0$, from Eq. (39) one obtains $l(0) = 0$. Further, to determine the dynamic surface tension, $\sigma(t)$, one uses the respective surface equation of state, $\sigma(\Gamma)$, cf. Table 1. This theoretical method is found to compare very well with experimental data for dynamic surface tension of sodium dodecylsulfate solutions measured by means of the MBP method [35].

The approach based on Eqs. (41)-(42) can be generalized to the case of micellar solutions, see Eqs. (76)-(78).
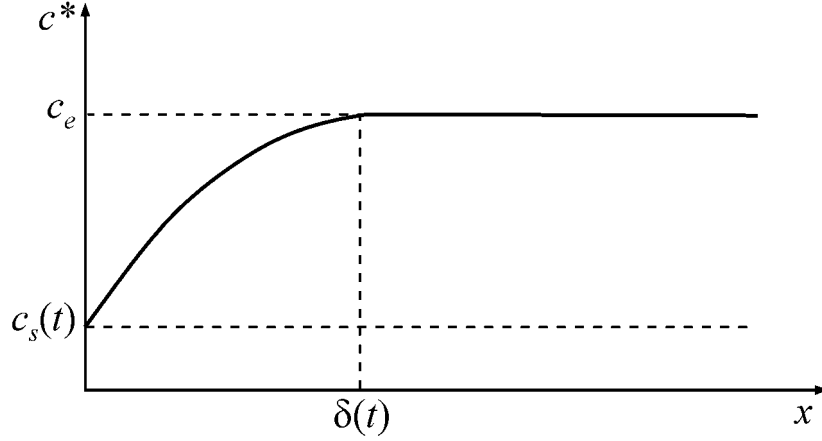
Fig. 2. The model profile c^* vs. x at a given moment t. $c_s(t)$ is the subsurface surfactant concentration; $\delta(t)$ is the point of smooth matching of the sine with constant, cf. Eq. (40).

C. Adsorption under barrier control

As mentioned above, the kinetics of adsorption is called *barrier limited* when the stage of surfactant transfer from the subsurface to the surface is much slower than the diffusion stage because of the existence of some kinetic barrier. This barrier can be due to steric hindrance, electrostatic repulsion or conformational changes accompanying the adsorption of the molecules. As the diffusion is the fast stage, the surfactant concentration in the solution should be uniform and equal to that at equilibrium: $c(x,t) = c_e =$ const. In such a case, the rate of increase of the adsorption, $\Gamma(t)$, is solely determined by the "jumps" of the surfactant molecules over the adsorption barrier separating the surface from the subsurface:

$$\frac{d\Gamma}{dt} = r_{\text{ad}}(c_s, \Gamma) - r_{\text{des}}(\Gamma). \tag{43}$$

Here r_{ad} and r_{des} are the rates of surfactant adsorption and desorption and , as usual, c_s is the surfactant subsurface concentration. (In a more general case of not too fast diffusion the subsurface concentration, c_s, can differ from the bulk concentration, c_e.) Thus the problem is reduced to the finding of appropriate expressions for $r_{\text{ad}}(c_s, \Gamma)$ and $r_{\text{des}}(\Gamma)$.

The first models of barrier controlled adsorption have been formulated by Doss [86] and modified by Ross [87], both starting with the concept of Bond and Puls [88]. Further developments have been achieved by Blair [89], Ward [90], Hansen and Wallace [91], and Dervichian [92]. Baret *et al.* [93-95] analyzed the balance of the adsorption $r_{\text{ad}}(c_s, \Gamma)$ and desorption $r_{\text{des}}(\Gamma)$ rates and derived various analytical expressions related to known equilibrium adsorption isotherms. In Table 2 we summarize the most frequently used

expressions for the rate of barrier limited adsorption, cf. Refs. [65,78,93-95]. In Table 2 K_{ad} and K_{des} are the rate constants of adsorption and desorption, respectively, $K_e = K_{ad}/K_{des}$ is the equilibrium constant of adsorption, and the other notation is the same as in Table 1 above.

In fact, Table 2 contains model expressions; each of them can be substituted in the right-hand side of Eq. (43) in order to calculate the rate of adsorption. In the simplest case of very fast diffusion, when $c_s = c_e.=$ const, the integration of Eq. (43) yields

$$\Gamma(t) = \Gamma_e + (\Gamma(0) - \Gamma_e)\exp(-K_{des}t) \qquad \text{(Henry and Freundlich)} \qquad (44)$$

$$\Gamma(t) = \Gamma_e + (\Gamma(0) - \Gamma_e)\exp\left[-(K_{des} + K_{ad}c_e/\Gamma_\infty)t\right] \qquad \text{(Langmuir)} \qquad (45)$$

Table 2. Kinetic models of reversible surfactant adsorption

	• **Total rate of surfactant adsorption**
Henry	$K_{ad}c_s - K_{des}\Gamma$
Langmuir	$K_{ad}c_s(1 - \Gamma/\Gamma_\infty) - K_{des}\Gamma$
Freundlich	$K_{ad}B_F(c_s/B_F)^m - K_{des}\Gamma$
Frumkin	$K_{ad}c_s\exp\left[\dfrac{\beta\Gamma_\infty}{kT}\left(\dfrac{\Gamma}{\Gamma_\infty}\right)^2\right]\left(1 - \dfrac{\Gamma}{\Gamma_\infty}\right) -$ $-K_{des}\Gamma\exp\left[\dfrac{\beta\Gamma_\infty}{kT}\left(\dfrac{\Gamma}{\Gamma_\infty}\right)^2 - \dfrac{2\beta\Gamma}{kT}\right]$
	• **Equilibrium constant of adsorption**
Henry	$K_e = \Gamma_\infty/B$
Langmuir	$K_e = \Gamma_\infty/B$
Freundlich	$K_e = \Gamma_F/B_F$
Frumkin	$K_e = \Gamma_\infty/B$

Similar, but much longer, expression related to the Frumkin isotherm (Table 2) can be also derived. In general, it turns out that in the case of *barrier* limited adsorption $(\Gamma_e - \Gamma)$ decays *exponentially*, in contrast with the case of *diffusion* limitation, in which $(\Gamma_e - \Gamma)$ decays proportionally to $t^{-1/2}$: compare Eqs. (44)-(45) with Eqs. (28)-(29). The same is true for the time dependence of the surface tension relaxation.

When the diffusion is not too fast, we deal with the more general case of *mixed* diffusion-barrier control, which has been studied by Baret [95]. The solution of the diffusion boundary problem in this case leads to the following equation

$$c_s = c_e - \left(\frac{4}{\pi D}\right)^{1/2} \int_0^t \frac{d\Gamma(t-\tau)}{dt} d\sqrt{\tau} \,, \tag{46}$$

which together with Eq. (43) forms an integro-differential system. A numerical analysis of this system has been performed in Ref. [96] by using the Henry and Langmuir models, as well as in Ref. [65] on the basis of the Frumkin model, cf. Table 2. Quite different model was proposed by Tsonopoulos *et al.* [97] and Yousef and McCoy [98], who treated the subsurface region as an independent bulk phase with appropriate properties. Adamczyk [99,100] and Filippov [78] generalized the model of mixed diffusion-barrier controlled adsorption and derived some useful approximate expressions. Balbaert and Joos [101] investigated the rheological aspect of the problem and demonstrated the applicability of the Boltzmann superposition principle to the quantitative description of repeatedly compressing and expanding adsorption layers of nonionic surfactants.

As an illustration below we give the solution of the mixed (diffusion-barrier) problem employing the Henry model to characterize the barrier (see Table 2). In fact, the Henry model is the only one which allows an exact analytical solution for $\Gamma(t)$:

$$\Gamma(t) = \Gamma(0) + \left(K_e c_e - \Gamma(0)\right)\left[F(\tau, b_2) - F(\tau, b_1)\right] \tag{47}$$

where $\tau = K_{des}t$ is dimensionless time, $b_{1,2} = \beta \pm (\beta^2 - 1)^{1/2}$ are dimensionless parameters, with $\beta = K_{ad}/(4DK_{des})^{1/2}$ being a dimensionless diffusion-kinetic ratio coefficient; the function F is defined as follows:

$$F(\tau, b) = \frac{1}{2b\sqrt{\beta^2 - 1}}\left[1 - \exp\left(b^2 \tau\right)\text{erfc}\left(b\sqrt{\tau}\right)\right] \tag{48}$$

This solution implies that the characteristic time of the mixed, diffusion-barrier controlled, adsorption is $t_{ch} = 4D/K_{ad}^2$. In other words, the diffusion controls the kinetics of adsorption when the time of the experiment is $t \gg t_{ch}$, whereas the barrier controls the adsorption when $t \ll t_{ch}$. In Fig. 3 the dependence of the dimensionless adsorption, Γ/Γ_e, on the dimensionless time τ, calculated by means of Eq. (47), is shown for various values of the parameter β. It is seen that the adsorption Γ is greater, when the diffusion is faster (at fixed barrier), which is related to the fact that for larger diffusivity D the value of the parameter β (denoted on the curves) is smaller.
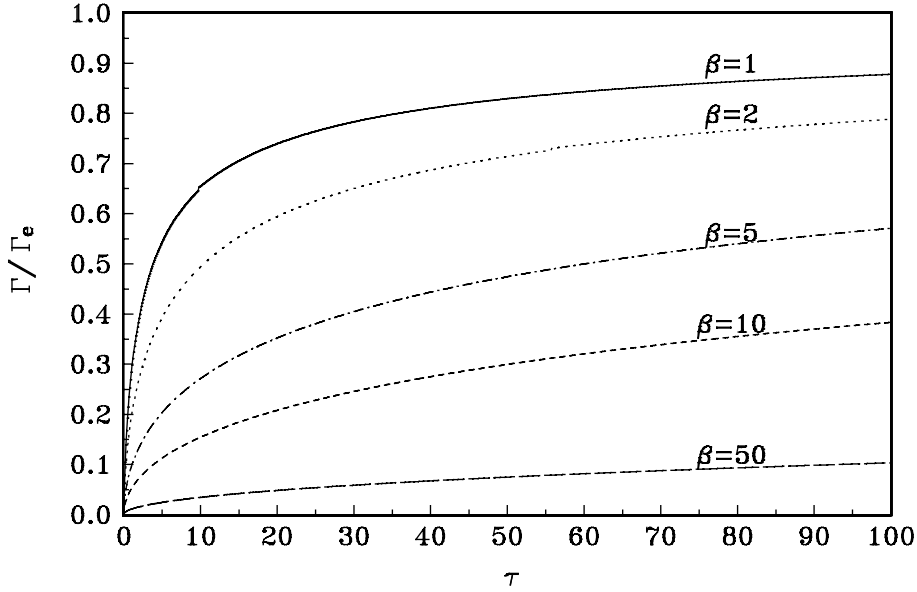
Fig. 3. Dependence of the dimensionless adsorption, Γ/Γ_e, on the dimensionless time τ, for various values of the parameter β.

D. Electro-diffusion control (adsorption of ionic surfactants)

Let us consider the process of adsorption of ionic surfactants at an quiescent ($\mathbf{v} = 0$) planar surface coinciding with the coordinate plane $x = 0$, see Fig. 4. In this case the equation of electro-diffusion, Eq. (18), reduces to

$$\frac{\partial c_i}{\partial t} = \frac{\partial}{\partial x}\left(D_i \frac{\partial c_i}{\partial x} + D_i \frac{q_i c_i}{kT} \frac{\partial \psi}{\partial x} \right) \qquad (i = 1, 2, \ldots, N) \tag{49}$$
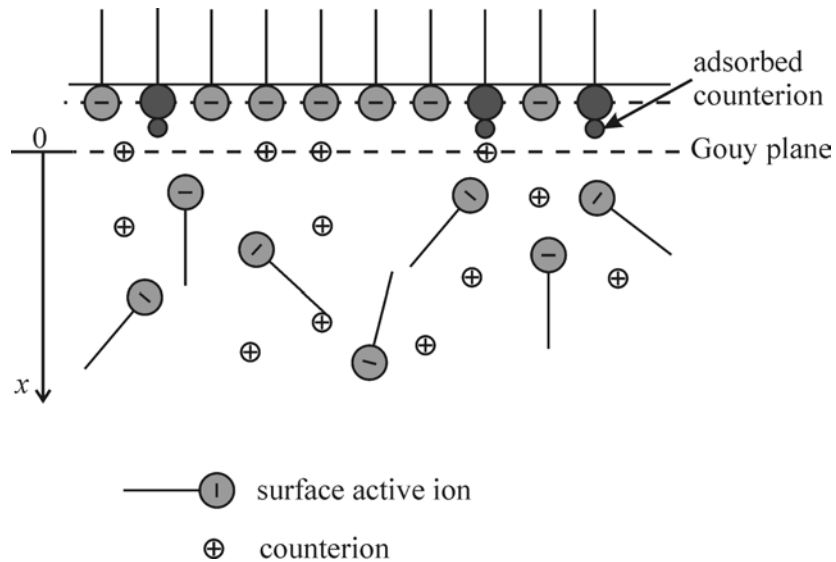

Fig. 4. Sketch of adsorption monolayer of anionic surfactant. The charge of the surface headgroups is partially neutralized by adsorbed counterions.

20

The concentration of the ionic species and the electric potential, ψ, are related by the Poisson equation [1-4]:

$$\varepsilon\varepsilon_0 \frac{\partial^2 \psi}{\partial x^2} = -\sum_{i=1}^{N} q_i c_i(x,t) \tag{50}$$

where ε and ε_0 are the dielectric constants of the medium and vacuum, respectively. Eqs. (49) and (50) form a *nonlinear* set of equations for determining the unknown functions $c_i(x,t)$ and $\psi(x,t)$.

The process of adsorption of ionic surfactants results in a continuous growing of the surface charge density and the surface potential with time. In its own turn, the presence of surface electric potential leads to the formation of an electric double layer inside the solution [1-4]. The charged surface repels the new-coming surfactant molecules (see Fig. 4), which results in a deceleration of the adsorption process. The respective boundary condition (for a uniform adsorption monolayer) stems from Eqs. (20) and (21) [102-105]:

$$\frac{d\Gamma_i}{dt} = D_i \left(\frac{\partial c_i}{\partial x} + \frac{q_i c_i}{kT} \frac{\partial \psi}{\partial x} \right)_{z=0} \qquad (i = 1,2,...,N_s) . \tag{51}$$

An additional relation follows from the condition for integral electroneutrality of the surfactant solution [2-4]:

$$\varepsilon\varepsilon_0 \left. \frac{\partial \psi}{\partial x} \right|_{z=0} = -\sum_{i=1}^{N_s} q_i \Gamma_i \tag{52}$$

The system formed by equations (49)-(52) has no analytical solution. Three types of approaches to this problem can be found in the literature: (i) *numerical* methods [21, 103, 106, 107], (ii) approximate analytical expression derived by using an assumption for *quasi-equilibrium regime* of surfactant adsorption [102-105], and (iii) exact asymptotic expressions for the case of *small deviations* from equilibrium [108, 109].

The *equilibrium* distribution of the ionic species in the electric double layer (which is the Boltzmann distribution) can be formally obtained by setting the left-hand side of Eq. (49) equal to zero:

$$c_{i,e}(x) = c_{i,\infty} \exp\left(-\frac{q_i \psi}{kT} \right) \qquad (i = 1,2,...,N) \tag{53}$$

Here $c_{i,\infty}$ denotes the surfactant concentration at large distance from the interface, where $\psi \equiv 0$. The characteristic extent of the electric double layer is determined by the Debye length, κ^{-1}, with $\kappa^2 = \sum_i (q_i^2 c_{i,\infty}) / (\varepsilon\varepsilon_0 kT)$. Dukhin *et al.* [102-105] presented a quasi-

equilibrium model of the ionic surfactant adsorption. They assumed that the characteristic time of the adsorption kinetics is much greater than the time of formation of the electric double layer, $t_{dl} = 1/(\kappa^2/D)$, as defined by Wagner [110]. Further, they simplified their task by separating the diffusion from the electric problem:

for $x > \kappa^{-1}$: common diffusion in electroneutral solution

for $x < \kappa^{-1}$: kinetic barrier against surfactant adsorption due to the surface charge.

In other words, these authors reduce the electro-diffusion problem to a mixed barrier-diffusion controlled problem (see the previous subsection). Such a simplification of the problem is correct when the ionic strength of solution is high enough in order to have small κ^{-1}, i.e. the electric double layer is thin enough to be modeled as a kinetic barrier. Then one can employ Eq. (46) to calculate the concentration at the "outer end" of the double layer (at $x = \kappa^{-1}$):

$$c_i\left(\kappa^{-1},t\right) = c_{i,\infty} - \left(\frac{4}{\pi D_i}\right)^{1/2} \int_0^t \frac{d\,\Gamma(t-\tau)}{d\,t}\,d\sqrt{\tau} \tag{54}$$

Finally an equation for barrier controlled adsorption is used [102-105]:

$$\frac{d\,\Gamma_i}{d\,t} = K_{i,\mathrm{ad}}\,c_i\left(\kappa^{-1},t\right) - K_{i,\mathrm{des}}\Gamma_i \qquad \left(i = 1,2,...,N_s\right)\,, \tag{55}$$

cf. Eq. (43). The rate constant of adsorption, $K_{i,\mathrm{ad}}$, depends on the surface electric potential. Asymptotic solutions of Eqs. (54) and (55) are presented in Ref. [105].

When the diffusion time has comparable magnitude with the time of formation of the electric double layer, the quasi-equilibrium model is not applicable. Lucassen *et al*. [111] and Joss *et al*. [112] established that mixtures of anionic and cationic surfactants diffuse as electroneutral combination in the case of small periodic fluctuations of the surface area; consequently, this process is ruled by the simple diffusion equation. The *electro*-diffusion problem was solved by Bonfillon *et al*. [113] for a similar case of small periodic surface corrugations related to the capillary-wave methods of dynamic surface tension measurement.

Another problem, which has been solved analytically, is related to the relaxation of the adsorption, $\Gamma(t)$, and the surface tension, $\sigma(t)$, of ionic surfactant solutions [108, 109]. In general, the long time asymptotics reads

$$\frac{\sigma_e - \sigma(t)}{\sigma_e - \sigma(0)} = \frac{\Gamma_e - \Gamma(t)}{\Gamma_e - \Gamma(0)} = \sqrt{\frac{t_r}{\pi t}} \qquad (t/t_r \gg 1) \tag{56}$$

where the subscript "*e*" denotes the equilibrium value of the respective quantity, and t_r is the relaxation time. In the case of a *nonionic* surfactant Eq. (56) can be deduced from Eq. (27) with

$$t_r = \frac{1}{D}\left(\frac{\partial \Gamma}{\partial c}\right)_e^2 \qquad \text{(nonionic surfactant)} \qquad (57)$$

where D is the diffusivity of the surfactant molecules.

In the case of *ionic* surfactant solution, *without* additional electrolyte, Eq. (56) holds again, but with the following specific expression for the relaxation time [108]:

$$t_r = \frac{1}{D_*}\left(\frac{\partial \Gamma}{\partial c_\infty}\right)_{\Phi_s}^2 \left[\frac{1}{2}+\frac{1}{2}\exp(-\Phi_s)+\lambda \exp\left(-\frac{3\Phi_s}{2}\right)\right]^{-2} \qquad \text{(ionic surfactant only)} \quad (58)$$

where $\Phi_s = |Ze\psi_s/kT|$ is the equilibrium value of the dimensionless surface potential (the surfactant is supposed to be a Z:Z electrolyte);

$$\frac{1}{D_*} \equiv \frac{1}{2}\left(\frac{1}{D}+\frac{1}{D_1}\right); \qquad \lambda \equiv \frac{\alpha\kappa}{2}\left(\frac{\partial \Gamma}{\partial c_s}\right)_e = \frac{\alpha\kappa}{2}\left(\frac{\partial \Gamma}{\partial c_\infty}\right)_{\Phi_s}\frac{1}{\exp(-\Phi_s)}. \qquad (59)$$

Here c_s is the subsurface concentration, D_1 is the diffusivity of the counterions and α is the apparent degree of dissociation of the surfactant adsorption monolayer accounting for the fraction of the surfactant ionizable groups which are not neutralized by adsorbed counterions, see Fig. 4. A formal transition to electroneutral surface, $\Phi_s \to 0$, $\alpha \to 0$, reduces Eq. (58) to Eq. (57) with an effective diffusivity D_* instead of D, cf. Eq. (59). The difference between D_* and D accounts for the electrolytic dissociation of the ionic surfactant.

In the case of *ionic* surfactant solution *with* added common electrolyte (like NaCl) Eq. (56) holds again, but along with another, more complicated, expression for the relaxation time [109]:

$$t_r = \frac{1}{D_{eff}}\left(\frac{\partial \Gamma}{\partial c_\infty}\right)_{\Phi_s}^2 \qquad \text{(ionic surfactant + electrolyte)} \qquad (60)$$

where D_{eff} is defined as follows

$$\frac{1}{D_{eff}} \equiv \left[\frac{x_s}{\sqrt{D_{**}}}+\frac{1-x_s}{2}\left(1+\exp(-\Phi_s)\right)\sqrt{\frac{1-x_s}{D}+\frac{x_s}{D_2}}\right]^2 \times \left[\frac{1}{2}+\frac{1}{2}\exp(-\Phi_s)+x_s\lambda\exp\left(-\frac{3\Phi_s}{2}\right)\right]^{-2}$$

$$\frac{1}{D_{**}} \equiv \frac{1}{2}\left(\frac{x_s}{D}+\frac{1}{D_1}+\frac{1-x_s}{D_2}\right); \qquad x_s \equiv \frac{c_{\text{surfactant}}}{c_{\text{surfactant}}+c_{\text{electrolyte}}} \qquad (61)$$

where D_2 is the diffusivity of the coions of the additional electrolyte. One can check that for $x_s = 1$, i.e. in the limiting case without additional electrolyte, Eq. (60) reduces to Eq. (58), as it should be expected. On the other hand, for $x_s \to 0$, i.e. for a great amount of added electrolyte, Eq. (60) reduces to the respective expression for nonionic surfactants, Eq. (57). In other words, it turns out that in solutions of high ionic strength the ionic surfactants diffuse and adsorb like nonionic surfactants.

E. Adsorption from Micellar Solutions

At concentrations above the critical micellization concentration (CMC) the kinetics of surfactant adsorption is strongly affected (accelerated) by the presence of micelles. In general, the micelles exist in equilibrium with the surfactant monomers in the bulk of solution (Fig. 5). A dilatation of the surfactant adsorption monolayer leads to a transfer of monomers from the subsurface to the surface, which causes a transient decrease of the subsurface concentration of monomers. The latter is compensated by disintegration of part of the micelles in the subsurface layer (Fig. 5). These processes are accompanied by diffusion transport of monomers and micelles driven by the concentration gradients.
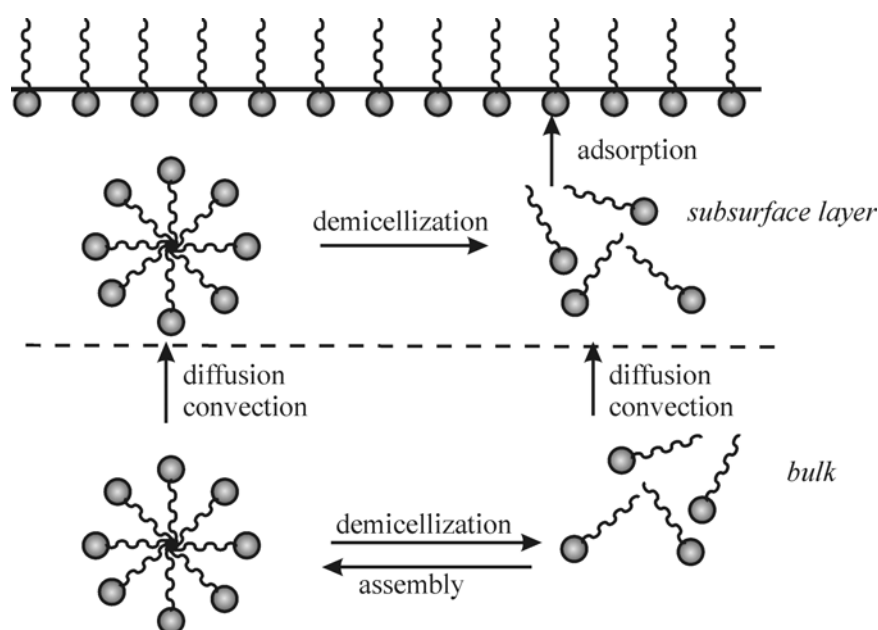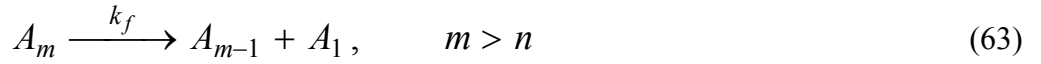

Fig. 5. In a vicinity of an expanded adsorption monolayer the micelles release monomers in order to restore the equilibrium surfactant concentration on the surface and in the bulk. The concentration gradients give rise to diffusion of micelles and monomers.

Aniansson *et al.* [114-117] have theoretically described the micelles as polydisperse species, whose growth or decay is determined by the reaction

$$A_i \underset{K_i^+}{\overset{K_i^-}{\leftrightarrow}} A_{i-1} + A_1 \qquad (i = 2,..., M) \tag{62}$$

where K_i^+ and K_i^- are, respectively, the rate constants of micelle growth and decay, and M is the aggregation number of the largest micelles. It should be noted, that the experiments on micellization show that the relaxation in a micellar solution is characterised by two relaxation times [115, 117], which can be interpreted in the following way. The decay of a micelle is considered as a consequence of *fast* and a *slow* process. The fast process is

$$A_m \xrightarrow{k_f} A_{m-1} + A_1, \qquad m > n \tag{63}$$

where k_f is the respective rate constant. In other words, for m greater than a certain value n a micelle can easily release a monomer and transform into micelle of aggregation number m-1 without destruction of the micellar aggregate. In contrast, the detachment of a monomer from a micelle with the *critical* aggregation number, $m = n$, leads to a break of the micelle into highly unstable fractions, which disintegrate to monomers. This is the slow process, which can be characterises by the equation

$$A_n \xrightarrow{k_s} n A_1 \tag{64}$$

Here k_s is the rate constant of the slow process, which can be c.a. 100 times smaller than k_f [115, 117].

Quantitatively, the presence of micelles influences the monomer concentration, $c_1(x,t)$, through the rate of monomer production due to micelle decay, see the source term R_1 in Eq. (18). The most general theoretical description, related to Eqs. (18) and (62), is based on the following set of equations:

$$\frac{\partial c_1}{\partial t} = D_1 \frac{\partial^2 c_1}{\partial x^2} - 2\left(K_2^+ c_1^2 - K_2^- c_2\right) - \sum_{i=3}^{M}\left(K_i^+ c_1 c_{i-1} - K_i^- c_i\right) \tag{65}$$

$$\frac{\partial c_i}{\partial t} = D_i \frac{\partial^2 c_i}{\partial x^2} + \left(K_i^+ c_1 c_{i-1} - K_i^- c_i\right) - \left(K_{i+1}^+ c_1 c_i - K_{i+1}^- c_{i+1}\right) \tag{66}$$

where $i = 2,3,..., M$ and $K_{M+1}^+ = K_{M+1}^- = 0$. What concerns the boundary conditions for Eqs. (65)-(66), we note that only surfactant monomers and none of the surfactant aggregates do adsorb at the interface. This leads to the following boundary conditions for the diffusion fluxes at the solution surface:

$$\frac{d\Gamma}{dt} = D_1 \frac{\partial c_1}{\partial x} \quad , \qquad \frac{\partial c_i}{\partial x} = 0 \qquad (i = 2, 3, ..., M) \tag{67}$$

It is a difficult task to solve Eqs. (65)-(67). That is the reason why some physical simplifications are usually made.

Most frequently used is the Lucassen [118] approach with *monodisperse* micelles (of aggregation number m); this approach is related to the studies of bulk micellization kinetics by Kresheck *et al.* [119], Muller [120], and Hoffmann *et al.* [121]. The model provides the following expressions for the source terms in Eq. (18):

$$R_1 = mK_d c_m - mK_a c_1^m, \qquad R_m = -K_d c_m + K_a c_1^m \tag{68}$$

where K_a and K_d are the rate constants of micelle assembly and decay. Using the same model, Miller [122] has solved numerically the respective diffusion equations for the monomers and the monodisperse micelles. The computations are carried out for the Henry's adsorption isotherm (which is not suitable for typical surfactants above CMC) and for the Langmuir adsorption isotherm. The numerical examples demonstrated that the adsorption relaxation in the presence of micelles is faster than the relaxation at concentrations close to CMC.

For concentrations close to CMC and for concentrations much above CMC the rate constant K_d can be related to the relaxation times of the slow and fast processes [123]:

$$K_d \approx k_s \quad \text{for} \quad c_m << c_1; \qquad K_d \approx \frac{m-n}{m} k_f \quad \text{for} \quad c_m \geq c_1 \tag{69}$$

- cf. Eqs. (63) and (64) above; usually $(m-n)$ is of the order of 5% of m.

In a number of works [124-126] the model of monodisperse micelles has been used to determine the diffusivity of the micelles. Joos and van Hunsel [127] have used this model to interpret experimental data for kinetics of adsorption obtained by the drop volume method. These authors have demonstrated that the data can be fitted by means of a simpler expression for R_1 and R_m, which are *linear* with respect to the concentration, see also Refs. [77, 128, 129]. In fact, every reaction mechanism reduces to a reaction of *"pseudo-first" order* for small deviations from equilibrium, see e.g. Ref. (130), Section 5.

The general problem based on Eqs. (65)-(67) has been solved by several authors, [130-134], for the special case of small deviations from equilibrium, and some analytical expressions have been derived. For example, the following expression for the relaxation of the surface tension of a micellar solution has been obtained [130]:

$$\frac{\sigma(t) - \sigma_e}{\sigma(0) - \sigma_e} = \frac{\Gamma_e - \Gamma(t)}{\Gamma_e - \Gamma(0)} = \frac{1}{g_1 - g_2} \left[E(g_1, \tau) - E(g_2, \tau) \right] \exp(-\tau) \tag{70}$$

where $E(g,\tau) = g\exp(g^2\tau)\mathrm{erfc}(g\sqrt{\tau})$, $\tau = t/td$, $\tau = t / t_d$, $g_{1,2} = [1 \pm (1 + 4\beta)^{1/2}]/2$, $\beta = t_d/t_m$, and

$$t_m = \left[K_d(1 + m^2 c_{m,e} / c_{1,e}) \right]^{-1}, \quad \text{and} \quad t_d = \left(\partial\Gamma / \partial c_1 \right)_e^2 / D_1 \tag{71}$$

are the characteristic relaxation times of micellization and diffusion, see Ref. [119]; as usual the subscript "e" denotes equilibrium values and m is the micelle aggregation number; K_d is a rate constant of micelle decay. Equation (71) is a generalization of Eq. (27) for the case of micellar solutions; indeed, the absence of micelles is equivalent to set $\beta = 0$; then $g_1 = 1$, $g_2 = 0$, and Eq. (70) reduces to Eq. (27).

The validity of Eq. (70) is restricted to the case of small deviations from equilibrium and quiescent surface ($\dot{\alpha} = 0$). A quantitative theory, which is not subjected to the latter two restrictions, can be developed by generalizing the approach of the model concentration profiles from Ref. [35]; this is done in Ref. [123]. In view of Eq. (68), the generalization of Eqs. (24)-(25) to micellar solutions reads:

$$\frac{\partial c_1}{\partial t} - \dot{\alpha}x\frac{\partial c_1}{\partial x} = D_1 \frac{\partial^2 c_1}{\partial x^2} + m K_d c_m - m K_a c_1^m, \quad (x > 0, t > 0) \tag{72}$$

$$\frac{\partial c_m}{\partial t} - \dot{\alpha}x\frac{\partial c_m}{\partial x} = D_m \frac{\partial^2 c_m}{\partial x^2} - K_d c_m + K_a c_1^m \quad (x > 0, t > 0) \tag{73}$$

$$\frac{d\Gamma}{dt} + \dot{\alpha}\Gamma = D_1 \frac{\partial c_1}{\partial x} \quad (x = 0, \quad t > 0) \tag{74}$$

In so far as one is interested in the time dependence of the *surface* properties, $\Gamma(t)$ and $\sigma(t)$, one can use appropriate *model* expressions for the monomer and micelle concentration profiles, $c_1^*(x,t)$ and $c_m^*(x,t)$. Thus the time consuming numerical integration of the *partial* differential equations (72)-(73) can be avoided. The functions $c_1^*(x,t)$ and $c_m^*(x,t)$ must satisfy the following integral condition for equivalence between the *real* and *model* concentration profiles, analogous to Eq. (39) [123]:

$$\int_0^\infty \left[1 - \frac{c_1^*(x,t)}{c_{1,e}} \right] dx = \int_0^\infty \left[1 - \frac{c_1(x,t)}{c_{1,e}} \right] dx \equiv l_1(t); \quad \int_0^\infty \left[1 - \frac{c_m^*(x,t)}{c_{m,e}} \right] dx = \int_0^\infty \left[1 - \frac{c_m(x,t)}{c_{m,e}} \right] dx \equiv l_m(t)$$

$$\tag{75a}$$

The model function $c_1^*(x,t)$ is defined [123] by an expression, which is completely analogous to Eq. (40). The model function $c_m^*(x,t)$ is defined by the expression

$$c_m^*(x,t) = \frac{1}{2}[c_{m,e} + c_{m,s}(t)] - \frac{1}{2}[c_{m,e} - c_{m,s}(t)]\cos\left(\frac{\pi x}{\delta_m}\right) \quad \text{for } x \le \delta; \tag{75b}$$

$$c_m^*(x,t) = c_{m,e} = \text{const} \qquad\qquad\qquad\qquad \text{for } x \ge \delta;$$

where $c_{m,s}(t)$ is the micelle subsurface concentration. The cosine in Eq. (75b) guarantees the fulfillment of the boundary condition, Eq. (67), for $i = m$. The model profiles $c_1^*(x,t)$ and $c_m^*(x,t)$ are visualized in Fig. 6.
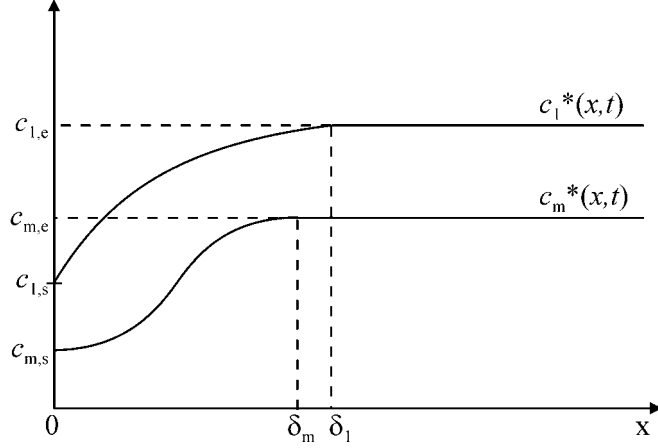

Fig. 6. Model concentration profiles, $c_1^*(x,t)$ and $c_m^*(x,t)$, of the free monomers and micelles at a given moment t. The interface is located at $x = 0$; $\delta_1(t)$ and $\delta_m(t)$ are the points of smooth matching of the sine (Eq. 40) and cosine (Eq. 75b) with the respective constant concentrations in the bulk.

Note the smooth matching of the cosine with the line $c_m = c_{m,e} = \text{const}$ at the point $x = \delta_m$. The positions of the matching points, $\delta_1(t)$ and $\delta_m(t)$, are determined from Eq. (75a). With the help of these model profiles the initial set of equations, Eqs. (72)-(74), reduces to the following relatively simple set of algebraic and ordinary differential equations [123]:

$$\Gamma(t) = c_{1,e}\, l_1(t) + c_{m,e}\, l_m(t) + \Gamma(0)/s(t) \tag{76}$$

$$\frac{dl_1}{dt} + \dot{\alpha}\, l_1 = \frac{(\pi - 2)D_1}{2\,l_1}\left(1 - \frac{c_{1,s}(t)}{c_{1,e}}\right)^2 - \frac{m}{c_{1,e}}\, Q(t) \tag{77}$$

$$\frac{dl_m}{dt} + \dot{\alpha}\, l_m = \frac{1}{c_{m,e}}\, Q(t) \tag{78}$$

$$\frac{dc_{m,s}}{dt} = \frac{\pi^2 D_m}{8\, c_{m,e}^2 l_m^2}\left[c_{m,e} - c_{m,s}(t)\right]^3 - K_d\, c_{m,s}(t) + K_a\, c_{1,s}^m(t) \tag{79}$$

28

$s(t)$ is the same as in Eq. (35). Equations (76)-(79), together with the adsorption isotherm, $c_{1,s}(\Gamma)$ (the latter can be any isotherm like those in Table 1), form a set of 5 equations for determining the 5 unknown functions, $\Gamma(t)$, $l_1(t)$, $l_m(t)$, $c_{1,s}(t)$ and $c_{m,s}(t)$. The term $Q(t)$ in Eqs. (77) and (78) is defined as follows:

$$Q = \frac{2K_a c_{1,e}^{m+1} l_1}{(\pi-2)(c_{1,e}-c_{1,s})} G_m\left(\frac{c_{1,s}}{c_{1,e}}\right) - K_d c_{m,e} l_m ;$$

$$G_m(\xi) \equiv \int_0^{\pi/2} \left\{ 1 - \left[\xi + (1-\xi)\sin\omega\right]^m \right\} d\omega$$

The system of Eqs. (76)-(79) can be solved numerically, and for the sake of convenience the special function $G_m(\xi)$ can be tabulated in the computer memory; a detailed description of the numerical procedure can be found in Ref. [123].

The above theory was applied for interpretation of dynamic surface tension data obtained with solutions of sodium dodecyl sulfate (SDS) by means of the MBP method. The empirical adsorption isotherm, $c_{1,s}(\Gamma)$, of SDS due to Tajima [29] was used with a value $m \approx 77$ of the mean aggregation number of the micelles. The best numerical fits of the data are shown in Fig. 7. Curves "a" and "b" correspond to surfactant concentrations below CMC; that is the reason why the respective data are processed by means of Eqs. (41)-(42).
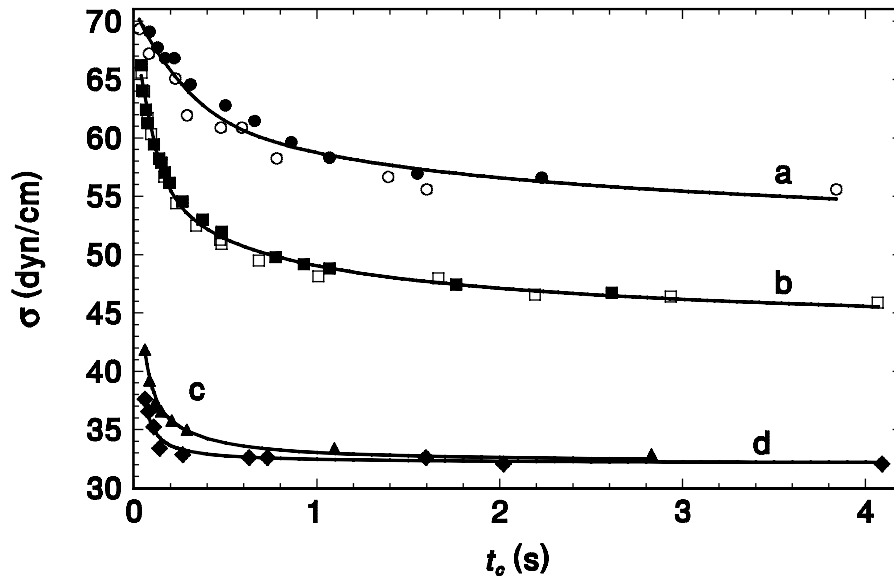

Fig. 7. Dynamic surface tension, σ, vs. the surface age, t_c, of submicellar (a,b) and micellar (c,d) solutions of SDS in the presence of 0.128 M NaCl measured by the maximum bubble pressure method at surfactant concentrations: (a) 0.2 mM, (b) 0.4 mM, (c) 1.5 mM, and (d) 2.0 mM. The solid and empty symbols correspond to different runs (after Ref. 84).

The calculated from the curves diffusion coefficient of the SDS monomers is $D_1 \approx 5 \times 10^{-6}$ cm²/s, which is close to the value determined by other authors [135]. This value of D_1 has been further used to fit the data for concentrations above CMC by means of Eqs. (76)-(79), see curves "c" and "d" in Fig. 7. Thus from the latter two curves one determines $K_d \approx 70$ s⁻¹ for the rate constant of micelle decay, which in view of Eq. (69) yields $k_f \approx 1400$ s⁻¹ for the characteristic time of the fast relaxation process of micellization.

F. Rheology of Adsorption Monolayers

All kinetic considerations in the previous sections have been based on the *mass* balance at the surface of a surfactant solution, Eq. (18). In the present subsection we proceed with the interfacial *momentum* balance and its physical implications. We consider below the theoretical description of the effects of elasticity and viscosity of surfactant adsorption monolayers, which are known as the effects of *Marangoni* [136] and *Boussinesq* [137]. These effects are important for many practical processes, such as dynamics and stability of emulsions and foams, spraying and atomization, flotation of ores, coating processes, etc. [28, 58, 138, 139]. The surface balance of the linear momentum can be expressed in the form [57, 58, 140, 142]:

$$\mathbf{n} \cdot \left[\mathbf{T}^{(1)} - \mathbf{T}^{(2)} \right] = \nabla_{II} \cdot \mathbf{T}_s + \Pi \hat{\mathbf{n}} \tag{80}$$

where $\mathbf{T}^{(1)}$ and $\mathbf{T}^{(2)}$ are the bulk stress tensors of the two neighboring phases, $\mathbf{n}$ is a running unit normal to the interface directed from phase 1 to phase 2; $\mathbf{T}_s$ is the *interfacial* stress tensor; Π is the disjoining pressure, which is operative *only* in thin liquid films; $\hat{\mathbf{n}}$ is the normal to the reference surface of the film, see Ref. [143].

The basis of the interfacial rheology is the *constitutive relation* for the interfacial stress tensor $\mathbf{T}_s$, which can be written as a sum of deviatoric and isotropic parts [137, 140, 144, 145]:

$$\mathbf{T}_s = (\sigma + \tau_{dil})\mathbf{I}_s + 2\eta_{sh}\left(\mathbf{D}_s - \frac{1}{2}\mathbf{I}_s \nabla_{II} \cdot \mathbf{v}_s \right) \tag{81}$$

where σ is the interfacial tension, τ_{dil} is *dilatational* interfacial viscous stress (see Eqs. 85 and 86 below), $\mathbf{I}_{II}$ is the surface unit tensor, η_{sh} is the interfacial *shear viscosity*; $\mathbf{D}_s$ is the surface *rate-of-strain* tensor, defined as

$$\mathbf{D}_s = \frac{1}{2}\left[\left(\nabla_{II}\mathbf{v}_s \right) \cdot \mathbf{I}_{II} + \mathbf{I}_{II} \cdot \left(\nabla_{II}\mathbf{v}_s \right)^T \right] \tag{82}$$

Eq. (81) is analogous to the constitutive relation of a *bulk* viscous fluid, see e.g. [146]; in particular, σ and η_{sh} are counterparts of the bulk isotropic pressure, P, and viscosity, η.

Historically, the necessity of accounting for special *surface* viscous effects, appeared after the experiments by Lebedev [147] and Silvey [148], which showed a contradiction with the theory of gravitational settling of emulsion droplets by Rybczynski [149] and Hadamar [150]. This contradiction was resolved by Boussinesq [137], who took into account the excess visco-elastic properties of the interface due to the presence of surfactant adsorption monolayer. Further, experimental methods for measurements of the surface viscosity have been developed.

F.1. Methods for measuring shear surface viscosity:

(i) The *deep-channel* surface viscometer is a frequently used experimental method for measuring interfacial *shear* viscosity owing to its sensitivity ($\eta_{sh} \geq 10^{-4}$ sp) and relatively simple analytical theory. The main drawback of this technique is the necessity of placing a small tracer particle within the interfacial flow field for tracking the central surface velocity. This may be particularly cumbersome with heavy oil systems, for which the particle may require several hours or more to execute a complete revolution, as well as with liquid-liquid systems, for which the placement of the particle at the interface may be difficult. For more details see refs. 58, 151-156.

(ii) The *disk* viscometers are generally less sensitive devices (compared to the channel method) for measuring interfacial shear viscosity (typically $\eta_{sh} \geq 10^{-2}$ sp) and exhibit a more complex flow field. The primary advantage of the disk techniques is their ability to directly measure the torsion stress. The exact placement of the disk at the interface and avoidance of contact angle anomalies are problematic issues with this techniques. The disk viscometers appear to be most useful for the measurements of η_{sh} of highly viscous interfacial adsorption layers [157-162].

(iii) The *knife-edge* viscometers are similar to the disk viscometers in most respects. A notable exception is the rotating wall knife-edge viscometer, which entails the measurement of the velocity of a tracer particle within the fluid interface and is quite sensitive to interfacial shear viscosity measurements, $\eta_{sh} \geq 10^{-5}$ sp. This device presently is the most promising surface viscometer. For more details see refs. 58, 153, 154, 158, 164-170.

(iv) A new method for the measurement of low surface shear viscosities is described in Refs. [171, 172]. This method is based on recording the sliding of a small spherical particle

down an inclined capillary meniscus formed in the vicinity of a vertical plate. The theory of the method employs accurate expressions for the capillary force exerted on the floating particle [173, 174], which is counterbalanced by the hydrodynamic drag force [175]. The experiment [172] gives values of the drag coefficient which are in good quantitative agreement with the hydrodynamic theory for pure liquids [175]. The addition of surfactant strongly increases the drag coefficient. The latter effect is used to measure the surface viscosity ($\eta_{sh} \geq 10^{-5}$ sp) of low molecular surfactants, such as SDS or Brij, whose surface viscosity is not accessible to the accuracy of the most of the other methods [173].

F.2. Dilatational surface viscosity

Interfacial dilatational stress is measured in processes of isotropic expansion (compression) of an interface. Such processes are realized in the maximum bubble pressure method [176-180], the oscillating bubble method [181-183], the pulsed drop method [184], and the drop expanding method [39, 83, 84, 185-187]. Because of the simple spherical symmetry Eq. (81), together with the projection of Eq. (80) along **n**, yields

$$\mathbf{T}_s = [\sigma(t) + \tau_{dil}(t)]\mathbf{I}_{II} = \frac{R(t)}{2}\left[P^{(1)} - P^{(2)}\right]\mathbf{I}_{II} \tag{83}$$

where $P^{(1)}$ and $P^{(2)}$ are the pressures inside and outside the droplet or bubble, and R is its radius. (At static conditions $\tau_{dil} = 0$ and Eq. (83) reduces to the known Laplace equation of capillarity.) For small deformations σ depends linearly on the *strain*, whereas τ_{dil} depends linearly on the *rate-of-strain*; therefore, the contributions of σ and τ_{dil} in Eq. (83) can be separated. In other words, σ and τ_{dil} account for the elastic and viscous effects accompanying the dilatation (compression) of the interface. In view of Eq. (17), for small deformations one can write:

$$\sigma = \sigma_e + E_G \varepsilon, \qquad \varepsilon \equiv \frac{\delta a}{a} \tag{84}$$

where E_G is the Gibbs elasticity, a is the area per surfactant molecule, and ε is the relative dilatation of the adsorption monolayer. There are two alternative expressions (constitutive relations) for the dilatational stress:

$$\tau_{dil} = \eta_{d,\alpha}\,\dot{\alpha}, \qquad \dot{\alpha} = \frac{1}{A}\frac{dA}{dt} \qquad \text{(Refs. 137, 140)} \tag{85}$$

where A is the *total* interfacial area, and

$$\tau_{dil} = \eta_{d,\varepsilon}\,\dot{\varepsilon}, \qquad \dot{\varepsilon} = \frac{1}{a}\frac{da}{dt} \qquad \text{(Refs. 83, 84)} \tag{86}$$

where $\eta_{d,\alpha}$ and $\eta_{d,\varepsilon}$ are coefficients of surface *dilational* viscosity. As illustrated in Fig. 8, for soluble surfactants $\dot{\varepsilon}$ is always smaller than $\dot{\alpha}$ because of the diffusion supply of surfactant molecules from the bulk of solution. In the limiting case of *slow* dilatation $\dot{\varepsilon} = 0$, even if $\dot{\alpha} \neq 0$, because the diffusion succeeds to saturate the surface with surfactant and there is no actual change in the density of the adsorption monolayer. In the other limit of *fast* dilatation the diffusive surfactant supply is negligible and $\dot{\alpha} \approx \dot{\varepsilon}$. For *insoluble* surfactants $\dot{\alpha} \equiv \dot{\varepsilon}$. From a physical viewpoint the definition (86) of surface dilational viscosity seems to be more reasonable because $\dot{\varepsilon}$ accounts for the *real* variation of the distance between the adsorbed molecules in the process of surface dilatation or compression [83, 84], cf. Fig. 8.
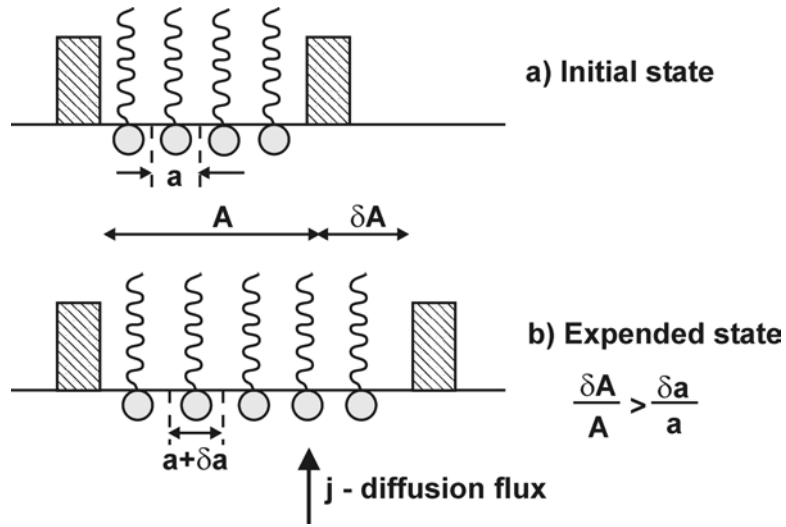

Fig. 8. The relative expansion of the area per molecule, *δa/a*, is smaller than the respective expansion of the total area, *δA/A*, because of the diffusion supply of surfactant molecules from the bulk of solution.

The analogue of $\eta_{d,\varepsilon}$ (or $\eta_{d,\alpha}$) in the three-dimensional (bulk) rheology is the so called "second viscosity", which is responsible for the decay of the intensity of sound in viscous fluids [146].

Using Eqs. (84)-(86) one can obtain from Eq. (83) two alternative forms for the variation of the isotropic surface stress:

$$\delta T_s = E_G\, \varepsilon + \eta_{d,\alpha}\, \dot{\alpha}, \qquad \text{or} \qquad \delta T_s = E_G\, \varepsilon + \eta_{d,\varepsilon}\, \dot{\varepsilon} \qquad (87)$$

In fact, δT_s can be directly determined by measuring the pressure inside the expanding droplet (bubble) and its radius; indeed, in view of Eq. (83) one can write

$$\delta T_s = \frac{1}{2}\left[R(t)\Delta P(t) - R(0)\Delta P(0)\right]; \qquad \Delta P \equiv P^{(1)} - P^{(2)} \qquad (88)$$

In addition, $\dot{\alpha}$ can be also experimentally determined from the recorded expansion of the droplet (bubble). However, for soluble surfactants it is very difficult to directly measure $\varepsilon(t)$

or $\dot{\varepsilon}(t)$. Instead, one can theoretically calculate $\varepsilon(t)$ from the equations of diffusion; combining Eqs. (27) and (37) one obtains [83]

$$\varepsilon = \int_0^{t_A(t)} \exp\left[\frac{t_A(t)-\theta}{t_r}\right] \text{erfc}\left[\sqrt{\frac{t_A(t)-\theta}{t_r}}\right] \frac{ds}{d\theta} d\theta, \quad t_A(t) \equiv \int_0^t s^2(t')dt' \qquad (89)$$

where t_r is the diffusion relaxation time, see Eqs. (57)-(60), and $s(t)$ (which is supposed to be known) is defined by Eq. (35).

It should be noted that for low molecular surfactants the viscous term in Eq. (87) is usually negligible. The relaxation of δT_s in this case is entirely determined by the *diffusion* relaxation of $\varepsilon(t)$, as given by Eq. (89), rather than to a real surface *viscous* relaxation related to $\eta_{d,\varepsilon}$ (or $\eta_{d,\alpha}$). Therefore, from such a relaxation process one can determine the diffusion relaxation time t_r, rather than the true surface dilatational viscosity, $\eta_{d,\alpha}$ or $\eta_{d,\varepsilon}$.

Eqs. (87)-(89) can be used to interpret data from expansion-relaxation experiments, see e.g. Refs. [39, 83, 84]. Fitting the experimental data for the interfacial dilatation one can in principle determine the Gibbs elasticity, E_G , the diffusion relaxation time, t_r, and the dilatational surface viscosity, $\eta_{d,\varepsilon}$ (or $\eta_{d,\alpha}$). . The latter is accessible to the accuracy of the aforementioned experimental techniques for high molecular surfactants and proteins; sometimes, $\eta_{d,\varepsilon}$ (or $\eta_{d,\alpha}$) can be determined also for low molecular anionic surfactants, but in the presence of multivalent counterions (like Ca^{2+} or Al^{3+}), which link neighboring surfactant headgroups.

A typical experiment can be constituted of the following three stages: (i) an initial formation of a saturated surfactant adsorption layer at the interface keeping the drop area constant for several hours, (ii) an expansion of the adsorption layer increasing the drop area for several seconds, and (iii) a relaxation of the expanded adsorption layer under a constant drop area. To illustrate the result of such an experiment, in Fig. 9 we present data from Ref. [83, 84] for bovine serum albumin (BSA) adsorption layers at decane-water interface. The influence of pH and the ionic strength on the rheological properties of BSA is investigated. In Fig. 9 the values of E_G, t_r and η_d (in this case $\eta_d = \eta_{d,\varepsilon} \approx \eta_{d,\alpha}$) are normalized by their values at pH = 5. The experimental data show that both the surface elasticity, E_G, and relaxation time, t_r, increase with increase of pH. The interfacial dilatational viscosity, η_d , exhibits a maximum at pH = 6. A similar peak of the interfacial shear viscosity of BSA at pH = 6 has been observed by Graham and Phillips [188] at petroleum ether-water interface. The results in Fig. 9 demonstrate a marked influence of the ionic strength on the rheological parameters.
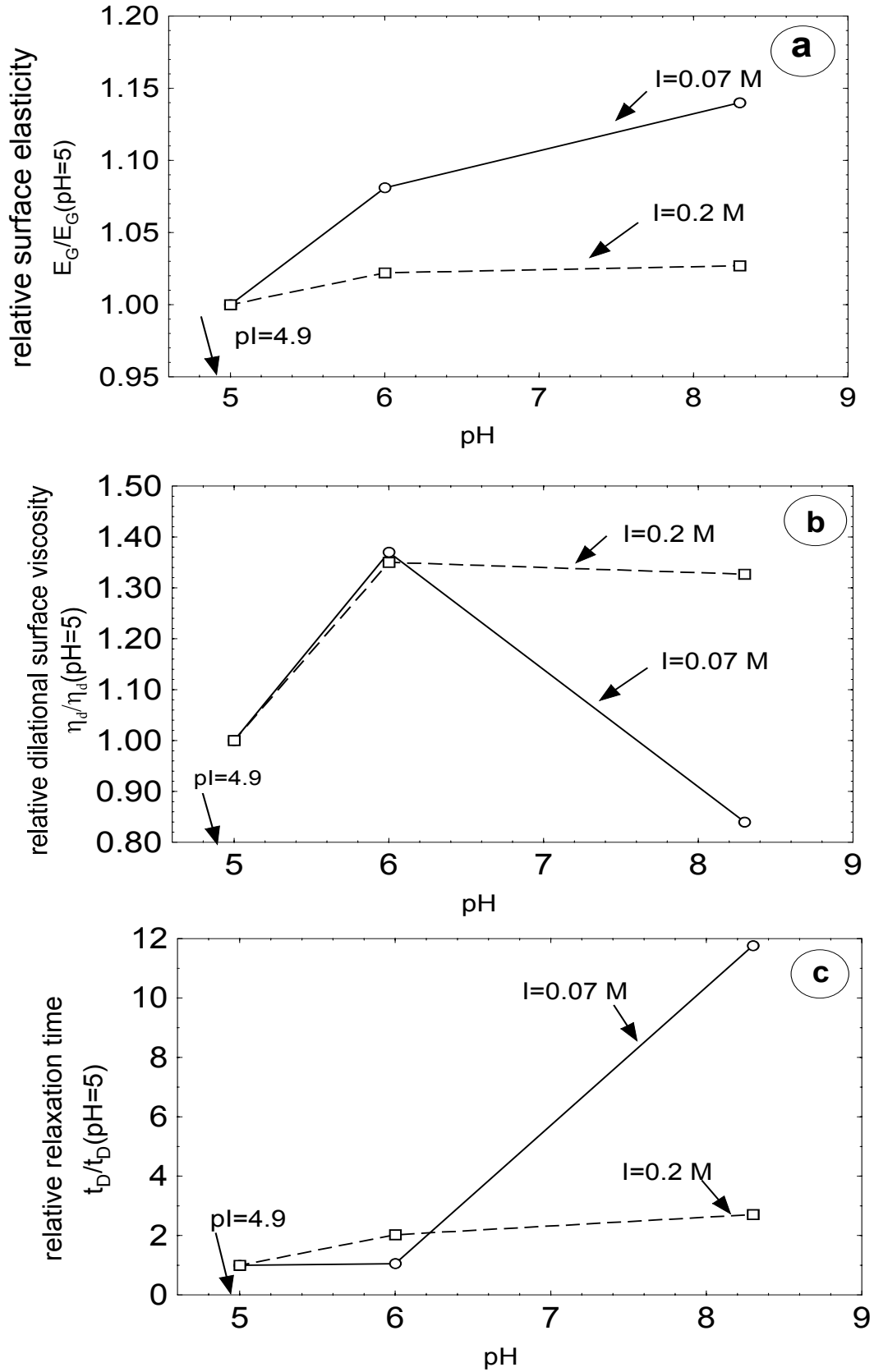
Fig. 9. Interfacial elasticity, E_G, diffusion relaxation time t_r, and interfacial dilatation viscosity, η_d, vs. pH of solutions of 0.0125 wt% BSA; the other phase is decane. pH is maintained by phosphate buffer; the ionic strength, I, is adjusted by NaCl. The droplet expansion method is applied (after Ref. 84).

One encounters the following difficulties in the interpretation of the data from the experiments with interfacial dilatation. As discussed in Ref. [58], the shear viscosity , η_{sh}, does not influence the total stress, δT_s, only for interfacial flow of perfect spherical symmetry. If the latter requirement is not fulfilled by a given experimental technique, its output data will be influenced by a mixture of dissipative effects (not only η_d, but also η_{sh} and t_r). The *apparent* interfacial viscosity thus determined is not a real interfacial property in so far as it depends on the specific method of measurement. For example, the apparent interfacial viscosity measured by the capillary wave methods [189-196] depends on the frequency; the apparent interfacial viscosity measured by the Langmuir trough method [197, 198] is a sum of the dilatational and shear viscosities ($\eta_d + \eta_{sh}$); for the methods employing non-spherical droplet deformation, like the spinning drop method [199-201], the apparent surface viscosity is a complex function of the dilatational and shear interfacial viscosities.

As an illustration let us consider the case of small droplet oscillating with a given frequency ω. By substituting the solution of the respective diffusion problem into Eq. (87) we derive the following relation

$$\delta T_s = \left[(E_G - q\omega\eta_d) + i(\omega\eta_d + qE_G) \right] \frac{(1-q)}{1+q^2} \delta\alpha; \quad \delta\alpha \equiv \int_0^t \dot{\alpha}\, dt \qquad (90)$$

where $i = \sqrt{-1}$ is the imaginary unit, and $q^{-1} = 1 + [2\omega tr]^{1/2}$ is a dimensionless parameter related to the characteristic diffusion time, t_r, cf. Eqs. (57)-(60), and the frequency of the droplet oscillations, ω. For high frequencies q is very small ($q \to 0$) and $\delta T_s/\delta a = EG + i\omega\eta_d$; i.e. the *real* and the *imaginary* parts of the derivative $\delta T_s/\delta a$ give the true Gibbs elasticity, E_G, and dilatational viscosity η_d. If the frequency is not so large, then the real and the imaginary parts of $\delta T_s/\delta a$ are combinations of E_G, t_r, η_d, and ω, see Eq. (90), which should not be termed "Gibbs elasticity" or "dilatational viscosity".

IV. FLEXURAL PROPERTIES OF SURFACTANT ADSORPTION MONOLAYERS

In the previous section we considered the response of a surfactant adsorption monolayer to *dilatation* and *shear* deformations. In addition, in the present section we will focus our attention on the properties of interfaces subjected to flexural deformations, i.e.

bending and *torsion*, see Fig. 10. Indeed, the interactions between the head-groups and the tails of adsorbed surfactant molecules lead to a non-zero work of bending or torsion.
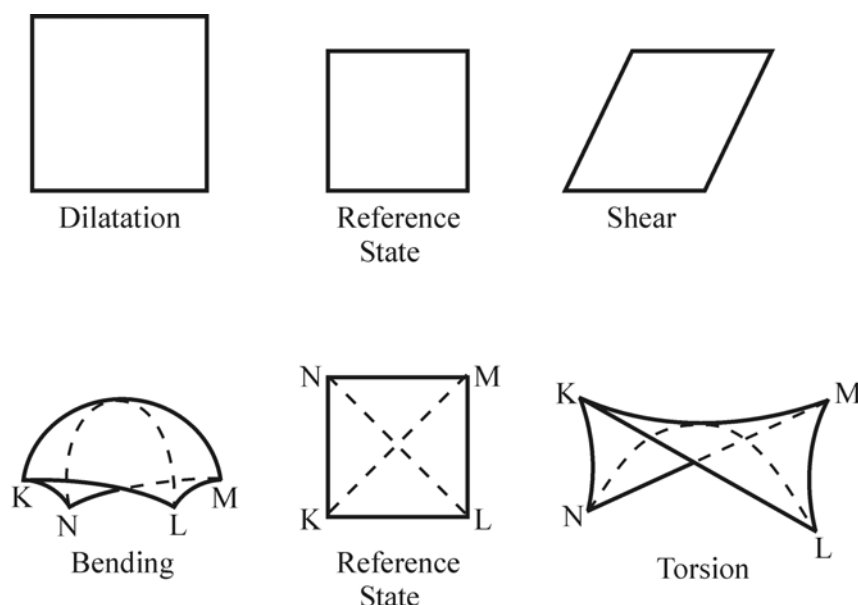

Fig. 10. Modes of deformation of a surface element: dilatation, shear, bending and torsion.

It should be noted that usually the energy of interfacial bending is much smaller than the energy of dilatation. That is the reason why the interfacial flexural properties are important for phase boundaries of low surface tension and/or high curvature, such as surfactant micelles, microemulsions, emulsions, as well as lipid monolayers, bilayers and biomembranes.

Below we first introduce the most general mechanical description of the surface moments (torques) exerted on the boundary between two fluid phases. Then we consider the thermodynamics of a curved interface (membrane) in terms of the work of flexural deformation. Next we specify the bending rheology by means of the model of Helfrich [202]. Finally we review the available expressions for the contributions of the electrostatic, steric and van der Waals interactions to the interfacial bending moment and curvature elastic moduli. These expressions relate the interfacial flexural properties to the properties of the adsorbed surfactant molecules.

A. Mechanical Description of a Curved Interface

Two approaches, mechanical and thermodynamical, exist for the theoretical description of general curved interfaces and membranes. The first approach originates from the classical theory of shells and plates, reviewed in Refs. (202, 204). The surface is regarded

as a two-dimensional continuum whose deformation is described in terms of the rate-of-strain tensor and the tensor of curvature. In addition, the forces and the force moments acting in the interface are expressed by the tensors of the interfacial stresses, $\underline{\sigma}$, and moments (torques), $\underline{\mathbf{M}}$. Figure 11 illustrates the physical meaning of the components of the latter two tensors. Usually they are expressed in the form

$$\underline{\sigma} = \mathbf{a}_\alpha \mathbf{a}_\beta \sigma^{\alpha\beta} + \mathbf{a}_\mu \mathbf{n} \sigma^{\mu(n)} \quad ; \quad \underline{\mathbf{M}} = \mathbf{a}_\alpha \mathbf{a}_\beta M^{\alpha\beta} \tag{91}$$

where Greek indices take values 1,2 (summation over repeated indices is supposed); $\mathbf{a}_1$, $\mathbf{a}_2$ are surface covariant base vectors and $\mathbf{n}$ is the running unit normal to the surface; $\sigma^{\mu(n)}$ ($\mu = 1,2$) are called transversal shear stresses.
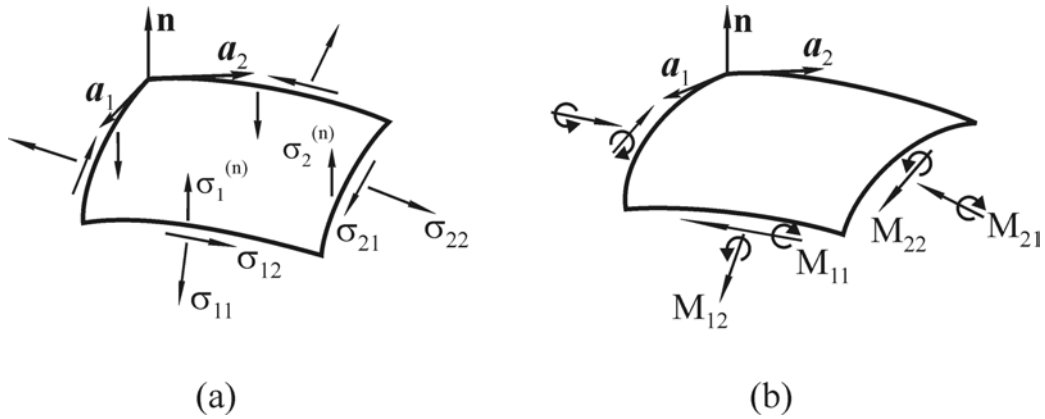

Fig. 11. Components of the tensors (a) of the surface stresses, $\underline{\sigma}$, and (b) of the surface moments (torques), $\underline{\mathbf{M}}$.

Tensor analysis and differential geometry can be applied in a straightforward manner to derive the interfacial balances of linear and angular momentum. The general formalism can be found in Refs. [203, 205]. Here we will only mention the results for the case of quasistatic processes (negligible angular acceleration), when $\sigma_{\alpha\beta}$ and $M_{\alpha\beta}$ are symmetric surface tensors which are both diagonal in the basis of principal curvatures. In these conditions the normal projection of the *angular* momentum balance is identically satisfied [205], and the tangential projection reads [203-206]:

$$\sigma^{\alpha(n)} = -M^{\alpha\beta}{}_{,\beta} \tag{92}$$

(the comma denotes covariant derivative). Obviously, the transversal shear resultants are connected with the presence of moments, which are not constant along the surface. The

normal and tangential projections of the *linear* momentum balance have the following form [203-206]:

$$b_{\alpha\beta}\sigma^{\alpha\beta} - M^{\alpha\beta}{}_{,\alpha\beta} = P_{II} - P_I \tag{93}$$

$$\sigma^{\alpha\beta}{}_{,\beta} + b^{\alpha}_{\beta}M^{\beta\gamma}{}_{,\gamma} = 0 \tag{94}$$

Here $b_{\alpha\beta}$ is the curvature tensor, and P_{II}–P_I is the pressure difference across the interface. Eq.(93) is the generalized Laplace equation, valid in the presence of moments. On spherical fluid interfaces $M^{\alpha\beta}{}_{,\alpha\beta} = 0$, due to the symmetry; the curvature tensor is isotropic, $b_{\alpha\beta} = Ha_{\alpha\beta}$ ($a_{\alpha\beta}$ are components of the surface metric tensor, and H is the mean curvature, $H = \frac{1}{2} a^{\mu\nu} b_{\mu\nu}$). Then Eq.(93) reduces to

$$2H\,\sigma = P_{II} - P_I \tag{95}$$

with σ being the scalar isotropic tension, $\sigma = \frac{1}{2} a_{\mu\nu}\sigma^{\mu\nu}$.

For a complete mechanical description of the surface one needs to specify expressions for the stresses and moments. This is usually done by postulating some constitutive relations between stress and strain, which pertain to a particular model for the rheological behavior of the interface. An example is the Scriven's constitutive relation [140] for $\underline{\sigma}$, see Eq. (81) above. In Section C below we discuss a constitutive relation for the tensor of the surface moments, $\underline{M}$. Before that we consider the thermodynamics of the curved interfaces.

B. Thermodynamics of Adsorption Monolayers and Membranes

The general thermodynamics of systems containing phase boundaries (including three-phase contact lines) is due to Gibbs [8]. The bulk phases in the idealized system are considered to be homogeneous up to sharp mathematical dividing surfaces. Excesses of all extensive properties (such as the internal energy, U, the free energy, F, the entropy, S, the number of molecules of the i-th component, N_i, etc.) are ascribed to the dividing surfaces. The latter are considered as separate surface phases with their own thermodynamic fundamental equations. The work for mechanical deformation is also taken into account. As far as the surface rate-of-strain tensor and the curvature tensor are two-dimensional, each of them has two independent scalar invariants. Therefore, one may distinguish exactly four independent

modes of surface deformation (Fig. 10): dilatation, shear, bending and torsion provide separate contributions to the mechanical work per unit area, δw^s [207-208]:

$$\delta w^S = \gamma \delta \alpha + \zeta \delta \beta + B \delta H + \Theta \delta D \tag{96}$$

This equation is valid locally, at each point of the surface. $\delta \alpha$ is the relative dilatation of a surface element dA, $\delta \alpha = \delta(\mathrm{d}A)/\mathrm{d}A$; $\delta \beta$ is connected with the deviatoric part of the surface rate-of-strain tensor [207] and characterizes the shear deformation. H and D are the mean and deviatoric curvatures:

$$H = \frac{1}{2}(c_1 + c_2) \quad ; \quad D = \frac{1}{2}(c_1 - c_2) \tag{97}$$

with c_1, c_2 being the two principal curvatures at a certain point of the surface. The coefficients γ and ζ have the meaning of *thermodynamic* interfacial tension and shearing tension, respectively. B and Θ represent the bending and torsion moments [207].

The basic idea of the local thermodynamic description, which is due to Gibbs [8], is to apply the fundamental equation of a uniform surface phase *locally*, i.e. for each elementary portion, dA, of the curved interface:

$$\delta(dU^S) = T\delta(dS^S) + \sum_i \mu_i \delta(dN_i^S) + (\delta w^S)dA \tag{98}$$

Here T and μ_i are temperature and chemical potentials; dU^s, dS^s and dN_i^s denote the excess surface internal energy, entropy and number of molecules of the i-th component, belonging to the elementary parcel dA; the symbol "δ" denotes infinitesimal variation due to the occurrence of a thermodynamic process in the system. Then one obtains [143]

$$\delta(dU^S) = \delta(u^S dA) = (\delta u^S + u^S \delta \alpha)dA \tag{99}$$

where u^s is the surface density of U^s. Similarly, one can derive

$$\delta(dS^S) = (\delta s^S + s^S \delta \alpha)dA \quad ; \quad \delta(dN_i^S) = (\delta \Gamma_i + \Gamma_i \delta \alpha)dA \tag{100}$$

with s^S and Γ_i being the surface densities of S^S and N_i^S, respectively. The substitution of Eqs. (96), (99) and (100) into Eq. (98), after some transformations, yields [207, 208]

$$\delta \omega^S = -s^S \delta T - \sum_i \Gamma_i \delta \mu_i + (\gamma - \omega^S)\delta \alpha + \zeta \delta \beta + B \delta H + \Theta \delta D \tag{101}$$

where $\omega^S \equiv u^S - Ts^S - \sum_i \mu_i \Gamma_i$ is the density of the surface excess grand thermodynamic potential.

Let us consider now fluid interfaces composed of chemical components, which are soluble in (and equilibrated with) the adjacent bulk phases. If a new piece of area is created at constant T, μ_i, β, H and D, this does not correspond to any change of the physical state of the interface. In such a case $(\partial \omega^S/\partial \alpha) = 0$ and from Eq.(101) one realizes that $\gamma = \omega^S$. Then Eq. (101) reduces to a generalized form of the Gibbs adsorption equation, cf. Eq. (1). It is now evident that the bending and torsion moments, B and Θ, are connected with the curvature dependence of the interfacial tension.

The mechanical and thermodynamical approaches are two complementary routes for description of interfaces and membranes of arbitrary shape. It is very important to find the connection between them, that is, to establish relations between the thermodynamically defined tensions and moments, γ, ζ, B, Θ (Eq. 96), and the mechanical tensors of stresses and moments, $\boldsymbol{\sigma}$, $\mathbf{M}$. This was done in Ref.[208] by direct calculation of δw^S in terms of purely mechanical quantities. The following results were obtained [208]:

$$\gamma = \sigma + \frac{1}{2}BH + \frac{1}{2}\Theta D \quad ; \quad \zeta = \eta + \frac{1}{2}BD + \frac{1}{2}\Theta H \tag{102}$$

$$\sigma = \frac{1}{2}(\sigma_1 + \sigma_2); \quad \eta = \frac{1}{2}(\sigma_1 - \sigma_2) \tag{103}$$

$$B = M_1 + M_2 \quad ; \quad \Theta = M_1 - M_2 \tag{104}$$

In the basis of principal curvatures the scalars σ_1, σ_2, M_1, M_2 are the eigenvalues of the tensors $\boldsymbol{\sigma}$ and $\mathbf{M}$, respectively. Thus, σ and η are isotropic and deviatoric tensions; B and Θ are isotropic (bending) and deviatoric (torsion) moments.

What is remarkable in Eq. (102) is that the mechanical tensions, σ, η, do not coincide with the thermodynamical ones, γ and ζ. In particular, this leads to ambiguity in defining what is called "fluid interface". It could be either $\zeta = 0$ (no work for shear), or $\eta = 0$ (isotropic surface stresses) - see more extended discussion in Ref. [205].

In the case of a spherical surface of radius a we have $B = 2M_1 = 2M_2$, $D = 0$, $H = -1/a$ and then Eqs. (95) and (102) yield

$$\gamma = \sigma - \frac{B}{2a} \quad ; \quad P_I - P_{II} = \frac{2\gamma}{a} + \frac{B}{a^2} \tag{105}$$

41

The second equation in (105) represents a form of the Laplace equation of capillarity. For the so called *surface of tension B* = 0 by definition [143, 208]; then $\gamma = \sigma$ and Eq. (105) coincides with Eq. (95). On the other hand, if the Gibbs dividing surface is defined as the *equimolecular dividing surface* (the surface for which the adsorption of solvent is equal to zero, see Ref. [8, 207], then *B* is not zero and the generalized Laplace equation should be used. It is interesting to note that for a *flat* intermolecular dividing surface *B* is proportional to the distance, δ_0, between the surface of tension and the intermolecular dividing surface [209, 210]:

$$B_0 = 2\gamma_0 \delta_0 \tag{106}$$

where the subscript "0" denotes flat interface ($H = 0$). Then by integrating Eq. (101) (with $\gamma = \omega^s$) for a deformation of pure bending one obtains the Tolman equation [8, 9, 211]

$$\gamma = \gamma_0 + B_0 H + O(H^2) = \gamma_0 \left[1 - \frac{2\delta_0}{a} + O\left(\frac{\delta_0^2}{a^2} \right) \right] \tag{107}$$

which expresses the physical dependence of surface tension on curvature. δ_0 is often called the Gibbs-Tolman parameter [9, 208].

C. Interfacial Bending Moment of Microemulsions

To illustrate the applicability of the above general expression let us consider a specified system: a microemulsion containing spherical droplets ($D = 0$, cf. Eq. 97). A typical microemulsion system contains the following components: water (*w*), oil (*o*), surfactant (*s*), cosurfactant (*c*) and neutral electrolyte (*e*) - see Fig. 12. We choose the dividing surface to be the equimolecular surface with respect to water, i.e. $\Gamma_w = 0$. Then at constant temperature *T* and chemical potential of the oil phase, μ_0, and for quasistatic processes without shear deformation ($\gamma = \omega^s$, $\delta\beta = 0$), Eq. (101) can be transformed to read [210]

$$d\left(\gamma + \Gamma_s \mu_s\right) = \mu_s d\Gamma_s - \Gamma_c d\mu_c - \Gamma_e d\mu_e + B dH \tag{108}$$

All differentials in the right-hand side of Eq. (108) are independent. Indeed, the number of the independent intensive parameters in the system under consideration is equal to the number of the components plus one [9]. Then from Eq. (108) one derives

$$\left(\frac{\partial B}{\partial \Gamma_s} \right)_{H, \mu_c, \mu_e} = \left(\frac{\partial \mu_s}{\partial H} \right)_{\Gamma_s, \mu_c, \mu_e} \tag{109}$$

The integration of Eq. (109) yields

$$B\left(H, \Gamma_s, \mu_c, \mu_e\right) = B_1\left(H, \mu_c, \mu_e\right) + B_s \tag{110}$$

where

$$B_s = \int_0^{\Gamma_s} \left(\frac{\partial \mu_s}{\partial H} \right)_{\Gamma_s, \mu_c, \mu_e} d\Gamma_s \tag{111}$$

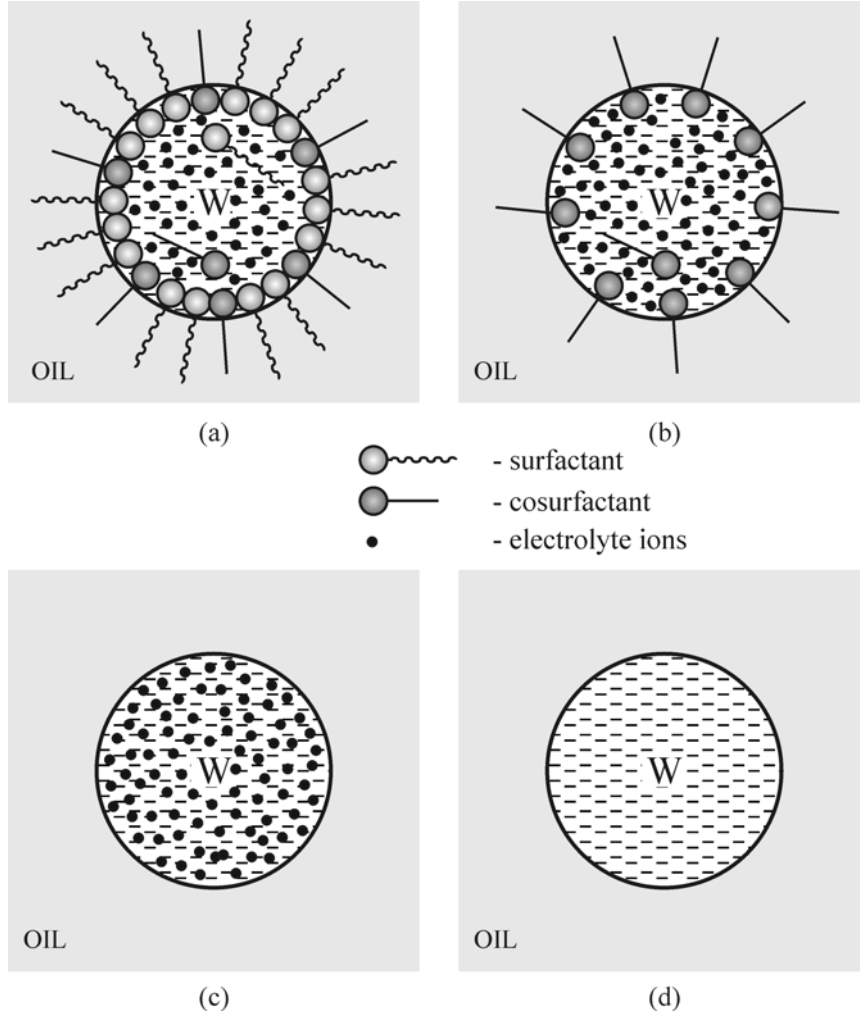is the contribution of the surfactant to the bending moment.

Fig. 12. Illustration of the derivation of Eq. (118) for a water-in-oil microemulsion droplet: (a) water, oil, surfactant, cosurfactant and electrolyte; (b) water, oil, cosurfactant and electrolyte; (c) water, oil and electrolyte; (d) pure water and oil phases.

The term $B_1(H, \mu_c, \mu_e)$ on the right-hand side of Eq. (110) represents the bending moment of the an imaginary emulsion drop in a system containing only cosurfactant and neutral electrolyte as solutes (Fig. 12b). For such a drop a counterpart of Eq. (108) holds:

$$d(\gamma + \Gamma_c \mu_c) = \mu_c d\Gamma_c - \Gamma_e d\mu_e + B_1 dH \tag{112}$$

From Eq. (112) one derives

$$\left(\frac{\partial B_1}{\partial \Gamma_c} \right)_{H, \mu_e} = \left(\frac{\partial \mu_c}{\partial H} \right)_{\Gamma_c, \mu_e} \tag{113}$$

By integrating Eq. (113) one obtains

$$B_1(H, \mu_c, \mu_e) = B_2(H, \mu_e) + B_c \tag{114}$$

Here

$$B_c = \int_0^{\Gamma_c(\mu_c)} \left(\frac{\partial \mu_c}{\partial H} \right)_{\Gamma_c, \mu_e} d\Gamma_c \qquad (115)$$

represents the contribution of the cosurfactant to the interfacial bending moment. $B_2(H,\mu_e)$ is the bending moment of an imaginary emulsion drop in a system containing neutral electrolyte of chemical potential μ_e in the aqueous phase (Fig. 12c). For such a system, instead of Eq. 112) one can write

$$d\left(\gamma + \Gamma_e \mu_e \right) = \mu_e d\Gamma_e + B_2 dH \qquad (116)$$

Then by analogy with Eq. (114) one derives

$$B_2\left(H, \mu_e \right) = B_p\left(H \right) + B_e \qquad (117)$$

where

$$B_e = \int_0^{\Gamma_e(\mu_e)} \left(\frac{\partial \mu_e}{\partial H} \right)_{\Gamma_e} d\Gamma_e$$

accounts for the contribution of the neutral electrolyte to the bending moment and $B_p(H)$ is the bending moment of an imaginary emulsion drop of surface curvature H in a system containing only pure aqueous and oil phase (Fig. 12d). A combination of Eq. (110), (114) and (117) leads to [210]

$$B = B_s + B_c + B_e + B_p \qquad (118)$$

In other words, the total interfacial bending moment of a typical microemulsion droplet can be represented as a superposition of four components.

Theoretical studies were devoted to calculation of the contributions of different intermolecular interactions in B. The results [210] show that the contributions due to the negative electrolyte adsorption (B_e) and the dipole moments of the adsorbed molecules are negligible compared to the contribution of the electric double layer and the van der Waals interaction. In Ref. [212] the contribution of the van der Waals interaction to the value of B for the phase boundary liquid-gas, as well as for the interface between pure water and hydrocarbon phases was calculated. For a planar interface it was found that the van der Waals contribution, B^{vw}, is of the order of 5×10^{-11} N, and tends to bend around the phase which has larger Hamaker constant. Electrostatic effects, due to adsorption of ionic surfactants, were shown to influence the bending moment considerably [210]. The Stern layer and the diffuse part of the double electric layer provide comparable contributions, both in the range 1-

2×10^{-11} N, having the same sign as B^{vw}. In addition, the bending moment can be connected with the experimentally measurable ΔV-potential across an interface [213], as well as with steric effects due to the surfactant tails and headgroups, see Refs. [214-221] and Section E below.

An approach to the calculation of γ and B is provided by the micromechanical theory, which is related to the statistical mechanics. In the special case of spherical interface one may use the expressions [208]:

$$\gamma = \frac{1}{3}\int_0^\infty \Delta P(r)\left(\frac{2a}{r}+\frac{r^2}{a^2}\right)dr, \quad B = \frac{2}{3}\int_0^\infty \Delta P(r)\left(\frac{a^2}{r}-\frac{r^2}{a}\right)dr \tag{119}$$

where r is the radial coordinate and $\Delta P(r) \equiv P_N - P_T$ expresses the anisotropy of the pressure tensor in the vicinity of the interface ($r = a$); P_N and P_T are the normal and tangential components of the latter tensor with respect to the interface [9, 209]. Theoretical expressions for $\Delta P(r)$ are available only for relatively simple systems. For example, supposing that only van der Waals forces are operative, a model expression for $\Delta P(r)$ is derived [212] for liquid-gas and oil-water interfaces. Fig. 13 represents the calculated curves ΔP vs r/a for benzene droplet in air and benzene droplet in water. A pronounced difference between the curves for liquid-gas and oil-water systems is seen: one maximum in the former case against maximum and minimum in the latter case. The respective values of B, calculated from the curves in Fig.13 by means of Eq. (119), are 3.5×10^{-11} N in the former case and 5.4×10^{-11} N in the latter case.
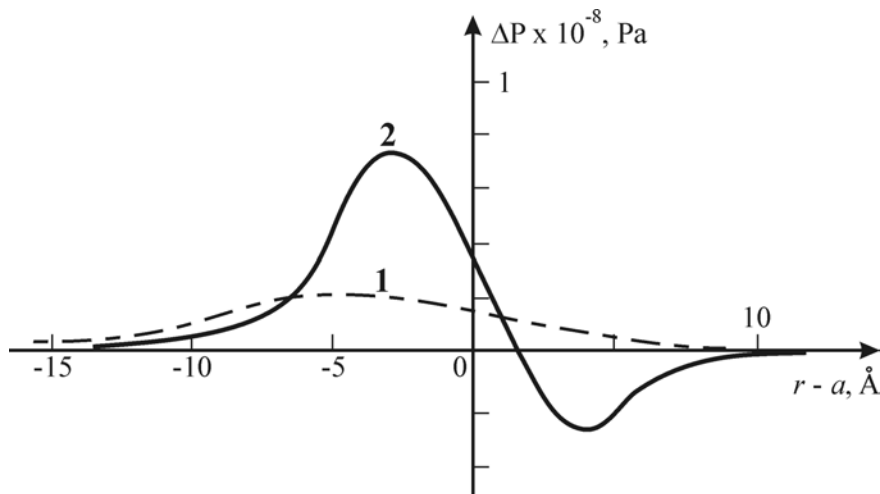

Fig. 13. Anisotropy, ΔP, of the pressure tensor vs. r - a, where r is the radial distance and $a = 100$ nm is the droplet radius: Curve 1 - benzene drop in air; Curve 2 - benzene drop in water.

D. Model of Helfrich for the Surface Flexural Rheology

In view of Eq. (96) the work of flexural deformation of an interface can be expressed in the form

$$dw_f = B\,dH + \Theta\,dD \tag{120}$$

Sometimes Eq. (120) is written in the alternative (but equivalent) form [222-225]

$$dw_f = C_1\,dH + C_2\,dK$$

where $K = H^2 - D^2$ is the Gaussian curvature, and the coefficients C_1 and C_2 are algebraically related to B and Θ [226]:

$$B = C_1 + 2C_2 H, \quad \Theta = -2C_2 D$$

In general, B and Θ (as well as C_1 and C_2) are curvature dependent. To determine the latter dependence one has to specify the flexural rheology of the interface. A frequently employed model of Helfrich [202] assumes that the work of flexural deformation can be written in the form

$$w_f = 2k_c\left(H - H_0\right)^2 + \bar{k}_c K \tag{121}$$

where H_0 is a parameter of the model called *the spontaneous curvature*, k_c and $\bar{k}_c$ are coefficients (moduli) of bending and torsion elasticity, supposedly constants. From Eqs. (120) and (121) one derives [205, 213, 226]

$$B = B_0 + 2\left(2k_c + \bar{k}_c\right)H, \quad \Theta = -2\bar{k}_c D \tag{122}$$

where

$$B_0 \equiv B\big|_{H=0} = -4k_c H_0 \tag{123}$$

is the bending moment of a planar interface. Note that Eq. (122) can be considered as truncated series expansions of B and Θ for small curvatures (small deviations from planarity). In addition, a comparison between Eqs. (106) and (123) shows that the quantities bending moment, B_0, spontaneous curvature, H_0, and Gibbs-Tolman parameter, δ_0, are closely related.

It should be noted also that the sign of the curvature H and the bending moment B is a matter of convention, which is specified by the definition of the *direction* of the running unit normal **n** to the surface. The general rule is that *positive B* tends to bend the interface around the *inner* phase (the phase for which **n** is an *outer* normal) [213].

Combining Eqs. (104), (122) and (123) one can derive an expression for the components of the tensor of the surface moments, **M** in the framework of the Helfrich model [205]:

$$M^{\alpha\beta} = 2\left[\left(k_c + \bar{k}_c\right)H - k_c H_0\right]a^{\alpha\beta} - \bar{k}_c b^{\alpha\beta} \tag{124}$$

- see Section A above for the notation. The substitution of Eq. (124) into Eq. (93) yields the form of the generalized Laplace equation in the framework of the Helfrich model [205]:

$$b_{\alpha\beta}\,\sigma^{\alpha\beta} - 2k_c\,a_{\alpha\beta}\,H^{,\alpha\beta} = P_{II} - P_I \tag{125}$$

It is interesting to note that $\bar{k}_c$ does not take part in Eq. (125).

Eq. (125) is often applied to analyze capillary waves of *small* amplitude u, for which Eq. (125) can be linearized; assuming isotropic surface tension, σ, from Eq. (125) one derives [205]:

$$\sigma\nabla_s^2 u - k_c\nabla_s^2\nabla_s^2 u = P_{II} - P_I \tag{126}$$

where ∇_s denotes surface gradient operator.

E. Physical importance of the bending moment and the curvature elastic moduli

In so far as the van der Waals, electrostatic and steric interactions can be treated as being independent, they give additive contributions to B and Θ [213]:

$$B = B^{vw} + B^{el} + B^{st}, \qquad \Theta = \Theta^{vw} + \Theta^{el} + \Theta^{st} \tag{127}$$

Then in accordance with Eq. (122) one can seek B_0, k_c and $\bar{k}_c$ in the form

$$B_0 = B_0^{vw} + B_0^{el} + B_0^{st}, \qquad k_c = k_c^{vw} + k_c^{el} + k_c^{st}, \qquad \bar{k}_c = \bar{k}_c^{vw} + \bar{k}_c^{el} + \bar{k}_c^{st} \tag{128}$$

The *van der Waals* contribution, B_0^{vw}, can be estimated by means of the expression

$$B_0^{vw} = \frac{8}{5}\pi^2\left(\alpha_{11}\rho_1^2 - \alpha_{22}\rho_2^2\right)\left(\frac{\gamma_0}{5\pi A_H}\right)^{1/2}, \qquad A_H = \pi^2\left(\alpha_{11}\rho_1^2 + \alpha_{22}\rho_2^2 - 2\alpha_{12}\rho_1\rho_2\right) \tag{129}$$

where γ_0 is the surface tension of the pure water-air or water-oil interface, A_H is the Hamaker constant, ρ_1 and ρ_2 are the number densities of the two neighboring phases, α_{ik} are the constants in the van der Waals potential: $u_{ik} = -\alpha_{ik}/r^6$; the subscripts "1" and "2" denote the phase inside and outside the fluid particle, respectively. In general, B_0^{vw} tends to bend around the phase, which has larger Hamaker constant [212]. For a oil-water interface Eq. (129) predicts $B_0^{vw} \approx 5 \times 10^{-11}$ N. Theoretical expressions for k_c^{vw} and $\bar{k}_c^{vw}$ are not available in the literature.

The contribution of the *steric* interaction can be related to the size and shape of the tails and headgroups of the surfactant molecules [214-221]. For example, the following expression was obtained [220] for such amphiphiles as the n-alkyl-poly(glycol-ethers), $(C_2H_4)_n(OCH_2CH_2)_mOH$:

$$B_0^{st} = -\frac{\pi^2 v^2 b \tilde{\varepsilon} kT}{4a_M^4}, \qquad k_c^{st} = \frac{\pi^2 v^3 bkT}{64a_M^5}(1 + 12\tilde{\varepsilon}^2) \qquad (130)$$

where $\tilde{\varepsilon} = (n-m)/(n+m)$ characterizes the asymmetry of the amphiphile, v is the volume of an amphiphile molecule, a_M is the interfacial area per molecule, k is the Boltzmann constant, b is a molecular length scale in the self-consistent field model used [220].

Expressions for the *electrostatic* components of the curvature elastic moduli, k_c^{el} and $\bar{k}_c^{el}$, in terms of the nonlinear double layer theory can be found in Ref. [227]. Contributions of "point dipoles", diffuse and Stern parts of the electric double layer in B_0 are evaluated in Ref. [210]. Alternatively, one can relate B_0^{el}, k_c^{el} and $\bar{k}_c^{el}$ to the surface Volta potential, ΔV, which is a directly measurable parameter [213]:

$$B_0^{el} = \frac{\varepsilon}{8\pi}(\Delta V)^2\left(1 + \frac{2s}{d}\right), \qquad (131)$$

$$k_c^{el} = \frac{\varepsilon d}{12\pi}(\Delta V)^2\left(1 + 3\frac{s}{d} + 3\frac{s^2}{d^2}\right), \qquad \bar{k}_c^{el} = -\frac{\varepsilon d}{24\pi}(\Delta V)^2\left(1 + 3\frac{s}{d} + 3\frac{s^2}{d^2}\right) \qquad (132)$$

where ε is the dielectric constant, d is the distance between the positive and negative charges, s is the distance between the surface charges and the Gibbs dividing surface (the position of the latter is a matter of choice), see Fig. 14. ΔV in Eqs. (131) and (132) must be substituted in CGSE-units, i.e. the value of ΔV in volts must be divided by 300. Note that ΔV expresses the change of the surface potential due to the presence of an adsorption monolayer. ΔV can be measured by means of the methods of the radioactive electrode or the vibrating electrode [10], which give the drop of the electric potential across the interface.

Eqs. (131) and (132) can be used (i) when there is an adsorption layer of zwitterions or dipoles, such as non-ionic and zwitterionic surfactants or lipids, at the interface; (ii) when the electrolyte concentration is high enough and the counterions are located in a close vicinity of the charged interface to form a "molecular capacitor"; (iii) when the surface potential is low: then the Poisson-Boltzmann equation can be linearized and the diffuse layer behaves as a molecular capacitor of thickness equal to the Debye screening length [228]. For example, taking experimental value for zwitterionic lipids [229], $\Delta V = 350$ mV, and assuming $\varepsilon = 78.2$,

$d = 5\text{Å}$, $s/d << 1$, from Eqs. (131) and (132) one calculates $B_0^{el} = 4.2 \times 10^{-11}$ N, $k_c^{el} = 1.4 \times 10^{-20}$ J and $\bar{k}_c^{el} = -0.7 \times 10^{-20}$ J.
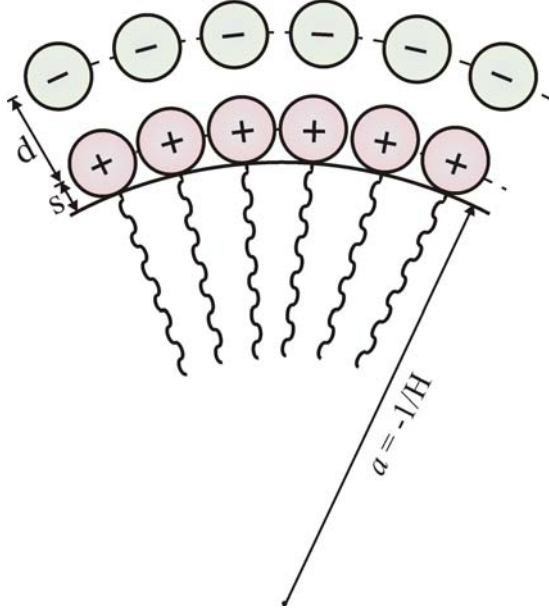

Fig. 14. Sketch of a "molecular capacitor" of thickness d at a spherical interface, which can be formed either by adsorbed zwitterionic surfactant, or by charged surfactant headgroups and their counterions; the Gibbs dividing surface of radius a is chosen to be the boundary between the aqueous and the hydrophobic phases.

Despite of the small values of the above parameters, it turns out that the energy of interfacial bending may considerably affect the droplet-droplet interactions in microemulsions and emulsions [230]. Indeed, the collisions between droplets of low interfacial tension is often accompanied by flattening of their surfaces in the zone of close contact, see Fig. 15, where the radius of the formed transient flat film is denoted by r. By using Eqs. (121) and (123) one may express the contribution of the bending energy to the droplet-droplet interaction, W_f, through the difference, Δw_f, between the droplet flexural energy after and before the film formation [230]:

$$W_f = 2\pi r^2 \Delta w_f = -2\pi r^2 B_0 H[1 + O(H/H_0)], \qquad (rH)^2 << 1 \quad (133)$$

Assuming $a = 1/H = 300$ nm, $r \approx a/50$, $|B_0| = 5 \times 10^{-11}$ N, and $H/H_0 << 1$, from Eq. (133) one calculates $|W_f| = 10$ kT. In other words, the bending effects can be important for the interaction between submicrometer emulsion droplets [230]. Since both the electrostatic and van der Waals components of B_0 tend to bend the interface around the oil phase, one can expect that $W_f < 0$ (attraction) for aqueous droplets in oil, whereas $W_f > 0$ (repulsion) for oil droplets in water. The existence of such an effect was established experimentally for water-in-oil microemulsions [231]: the observed formation of doublets of droplets can be attributed to the effect of $W_f < 0$.
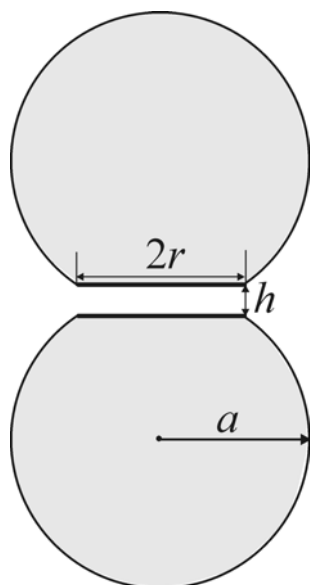
Fig. 15. Flat thin film of radius r and thickness h formed between two colliding fluid particles; the spherical part of the particle surface has radius a.

By means of similar considerations one can deduce [230] that an emulsion containing microemulsion droplets in the continuous phase should be more stable than an emulsion containing microemulsion droplets in the disperse phase, as it is observed experimentally [232].

Recently, the effect of the interfacial bending moment (or the spontaneous curvature, $H_0 = -B_0/(4k_c)$, see Eq. 123) was found to be important for the interaction between integral proteins incorporated in lipid membranes [233].

V. THIN LIQUID FILMS STABILIZED BY SURFACTANTS

In addition to the previous sections (dealing with *single* interfaces) in the present section we consider a *couple* of interfaces interacting across a thin liquid film. The presence of surfactants has a crucial role for the properties of the thin liquid films, which are constituent units of foams and some emulsions. Moreover, the *adsorption* of surfactants modifies the surfaces of solid or fluid particles in the colloidal dispersions and thus strongly affects the stability of the disperse systems. The presence of surfactant *micelles* also affects the stability of colloids.

In this section we consider the properties of *equilibrium* thin liquid films. Section VI is devoted to the *surface forces* of intermolecular origin acting in the liquid films or between the particles in dispersions. Finally, in Sections VII - IX we describe the role of surfactants in

the *hydrodynamic processes* in liquid films and dispersions, which are coupled with convective and diffusion transfer of surfactant.

A. Thermodynamic Description of a Thin Liquid Film

From a *mathematical* viewpoint a film is thin when its thickness is much smaller than its dimension in lateral direction. From a *physical* viewpoint a liquid film formed between two macroscopic phases is *thin* when the energy of interaction between the two phases across the film is not negligible. The specific forces causing the interactions in a thin liquid film are called *surface forces* [2-4].

In Fig. 16 a sketch of plane-parallel liquid film of thickness h is presented. The liquid in the film exists in contact with the bulk liquid in the *Plateau border*. The film is symmetrical, i.e. it is formed between two *identical* fluid particles (drops, bubbles) of internal pressure P_2. The more complex case of non-symmetrical and curved films is reviewed elsewhere [143-234].
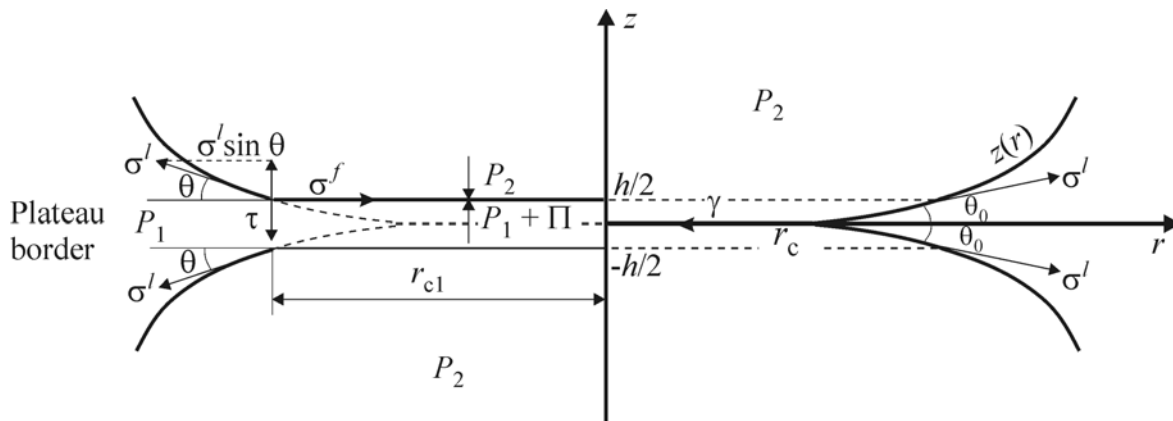

Fig. 16. The "detailed" and "membrane" models of a thin liquid film, on the left- and right-hand side, respectively.

Two different, but supplementary, approaches (models) are used in the macroscopic description of a thin liquid film. The first of them, the "membrane approach", treats the film as a membrane of zero thickness and *film tension*, γ, acting tangentially to the membrane - see the right-hand side of Fig. 16. In the "detailed approach", the film is modeled as a homogeneous liquid layer of thickness h and surface tension σ^f. The pressure P_2 in the fluid particles is larger than the pressure, P_1, of the liquid in the Plateau border. The difference $P_c = P_2 - P_1$ represents the capillary pressure of the liquid meniscus. By making the balance of the forces acting on a plate of unit width along the y-axis and height h placed normally to the film at $-h/2 < z < h/2$ (Fig. 16) one derives the Rusanov [235] equation:

51

$$\gamma = 2\sigma^f + P_c h \qquad (134)$$

Eq. (134) expresses a condition for equivalence between the membrane and detailed models with respect to the *lateral* force. To derive the *normal* force balance one considers a parcel of unit area from the film surface in the detailed approach. Since the pressure in the outer phase P_2 is larger than the pressure inside the liquid, P_1, the mechanical equilibrium at the film surface is ensured by the action of an additional *disjoining pressure*, $\Pi(h)$ representing the surface force per unit area of the film surfaces [236]

$$\Pi(h) = P_2 - P_1 = P_c \qquad (135)$$

- see the left hand side of Fig. 16. Note, that Eq. (135) is satisfied only at equilibrium; at non-equilibrium conditions the viscous force can also contribute to the force balance per unit area of the film. In general, the disjoining pressure, Π, depends on the film thickness, h. Note that $\Pi > 0$ means repulsion between the film surfaces, whereas $\Pi < 0$ means attraction.

A typical $\Pi(h)$-isotherm is depicted in Fig. 17a. (The shape of the curve in Fig. 17a is discussed in Section VI.A below.) One sees that the equilibrium condition, $\Pi = P_c$, can be satisfied at three points shown in Fig. 17a. Point 1 corresponds to a film, which is stabilized by the double layer repulsion; sometimes such a film is called the "primary film" or "common black film". Point 3 corresponds to unstable equilibrium and cannot be observed experimentally. Point 2 corresponds to a very thin film, which is stabilized by the short range repulsion; such a film is called the "secondary film" or "Newton black film". Transitions from common to Newton black films are often observed with foam or emulsion films [237-240].

In the framework of the membrane approach (Fig. 16) the film can be treated as a single surface phase, whose Gibbs-Duhem equation reads [143, 241]:

$$d\gamma = -s^f \, dT - \sum_{i=1}^{k} \Gamma_i \, d\mu_i \qquad (136)$$

where γ is the film tension, T is temperature, s^f is excess entropy per unit area of the film, Γ_i and μ_i are the adsorption and the chemical potential of the i-th component. The Gibbs-Duhem equations of phases 1 and 2 read

$$dP_\chi = s_v^\chi \, dT + \sum_{i=1}^{k} n_i^\chi \, d\mu_i, \qquad \chi = 1, 2 \qquad (137)$$

where s_v^χ and n_i^χ are entropy and number of molecules per unit volume, and P_χ is pressure ($\chi = 1, 2$).
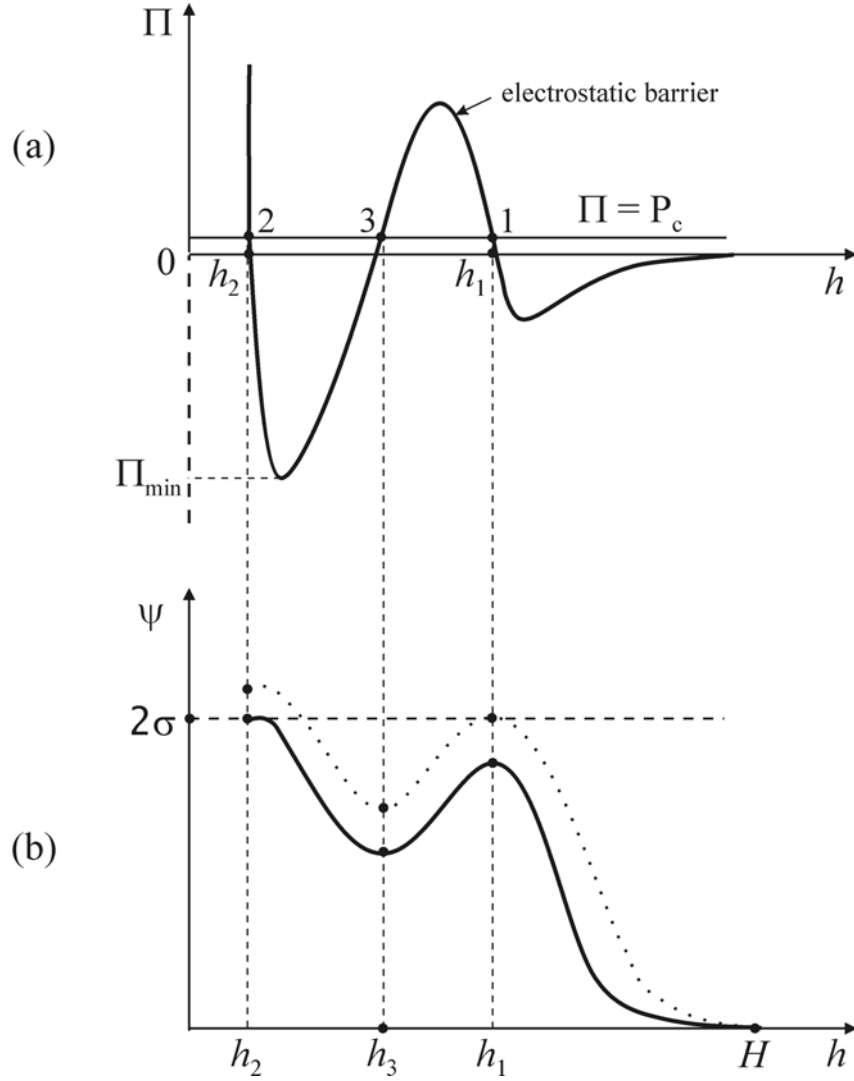
Fig. 17. (a) Sketch of a typical DLVO isotherm of the disjoining pressure, $\Pi(h)$, and of the resulting $\psi(h)$-curve (b) calculated by means of Eq. (167).

Having in mind that $P_c = P_2 - P_1$ from Eq. (137) one can derive an expressions for dP_c. Multiplying this expression by h and subtracting the result from the Gibbs-Duhem equation of the film, Eq. (136) one obtains [241]

$$d\gamma = -\tilde{s}\,dT + h\,dP_c - \sum_{i=1}^{k} \tilde{\Gamma}_i\,d\mu_i \tag{138}$$

where

$$\tilde{s} = s^f + \left(s_v^2 - s_v^1\right)h\,, \qquad \tilde{\Gamma}_i = \Gamma_i + \left(n_i^2 - n_i^1\right)h\,, \qquad i = 1,\ldots,k \tag{139}$$

To specify the model one needs an additional equation to determine the multiplier h. For example, let this equation be

$$\tilde{\Gamma}_1 = 0 \tag{140}$$

Eq. (140), in view of Eq. (139), requires h to be the thickness of a liquid layer from phase 1, containing the same amount of component 1 as the real film [242, 243]. This thickness is called the thermodynamic thickness of the film [243]. It can be of the order of the real film thickness if component 1 is chosen in an appropriate way, say the solvent in the film phase.

Combining Eqs. (135), (136) and (140) one obtains [242]

$$d\gamma = -\tilde{s}dT + hd\Pi - \sum_{i=2}^{k}\tilde{\Gamma}_i d\mu_i \tag{141}$$

A corollary of Eq. (141) is the Frumkin [244] equation

$$\left(\frac{\partial\gamma}{\partial\Pi}\right)_{T,\mu_2,\dots,\mu_k} = h \tag{142}$$

Eq. (142) predicts a rather weak dependence of the film tension γ on the disjoining pressure, Π, in equilibrium thin films (small h). The substitution of Eqs. (134) and (135) into Eq. (141) yields [243]

$$2d\sigma^f = -\tilde{s}dT - \Pi dh - \sum_{i=2}^{k}\tilde{\Gamma}_i d\mu_i \tag{143}$$

From Eq. (143) one can derive the following useful relations [242]

$$2\left(\frac{\partial\sigma^f}{\partial h}\right)_{T,\mu_2,\dots,\mu_k} = -\Pi \tag{144}$$

$$\sigma^f(h) = \sigma^l + \frac{1}{2}\int_h^\infty \Pi(h)\,dh \tag{145}$$

with σ^l being the surface tension of the bulk liquid. In particular, Eq. (145) allows calculation of the film surface tension (and the film tension) when the disjoining pressure isotherm, $\Pi(h)$, is known.

The above thermodynamic equations are in fact corollaries from the Gibbs-Duhem equation of the membrane approach Eq. (136). There is an equivalent and complementary approach, which treats the two film surfaces as separate surface phases with their own fundamental equations [235, 242, 245], thus for a flat symmetric film one postulates.

$$dU^f = TdS^f + 2\sigma^f dA + \sum_{i=1}^{k}\mu_i dN_i^f - \Pi A dh, \tag{146}$$

where A is area; U^f, S^f and N_i^f are excess internal energy, entropy and number of molecules ascribed to the film surfaces. Compared with the fundamental equation of a simple surface phase [9] Eq. (146) contains an additional term, $\Pi A dh$, which takes into account the

dependence of the film surface energy on the film thickness. Eq. (146) provides an alternative thermodynamic definition of the disjoining pressure:

$$\Pi = -\frac{1}{A}\left(\frac{\partial U^f}{\partial h}\right)$$

(147)

B. Contact Line, Contact Angle and Line Tension

B.1. Force balance at the contact line

The thin liquid films formed in foams or emulsions exist in a permanent contact with the bulk liquid in the Plateau border, encircling the film. From a macroscopic viewpoint, the boundary between film and Plateau border is treated as a three-phase contact line: the line, at which the two surfaces of the Plateau border (the two concave menisci sketched in Fig. 16) intersect at the plane of the film - see the right-hand side of Fig. 16. The angle, θ_0, subtended between the two meniscus surfaces, represents the thin film contact angle.

The interactions between the neighboring phases in a close vicinity of the contact line lead to the appearance of excess energy per unit length of the contact line. The latter is ascribed to the contact line as an effective line tension, κ, acting tangentially to the line [8]. For a curved contact line of radius r_c the line tension gives rise to a contribution of magnitude $\sigma_K = \kappa/r_c$ in the balance of the surface tensions at the contact line [246-251]. As a force (per unit length) σ_K is directed toward the center of curvature of the contact line. Thus, the force balance at the periphery of a symmetrical flat film with circular contact line, like those depicted in Fig. 16, reads [252]

$$\gamma + \frac{\kappa}{r_c} = 2\sigma^l \cos\theta_0 ,$$

(148)

There are two film surfaces and two contact lines in the detailed approach - see the left-hand side of Fig. 16. They can be treated thermodynamically as linear phases and an one-dimensional counterpart of Eq. (146) can be postulated [252]:

$$dU^L = TdS^L + 2\widetilde{\kappa}dL + \sum_i \mu_i dN_i^L + \tau dh$$

(149)

Here U^L, S^L and N_i^L are linear excesses, $\widetilde{\kappa}$ is the line tension in the detailed approach and

$$\tau = \frac{1}{L}\left(\frac{\partial U^L}{\partial h}\right)$$

(150)

is an one-dimensional counterpart of the disjoining pressure - cf. Eq. (147). The quantity τ, called the *transversal tension*, takes into account the interaction between the two contact lines. For the case of a flat symmetric film the tangential and normal projections of the force balance at the contact lines read (see the left-hand side of Fig. 16) [252]:

$$\sigma^f + \frac{\widetilde{\kappa}}{r_{c1}} = \sigma^l \cos\theta \tag{151}$$

$$\tau = \sigma^l \sin\theta \tag{152}$$

Note that in general $\theta \neq \theta_0$ - see Fig. 16. Besides, both θ_0 and θ can depend on the radius of the contact line due to line tension effects. In the case of straight contact line from Eqs. (145) and (151) one derives [243]

$$\cos\theta\big|_{r_{c1}=\infty} = \frac{\sigma^f}{\sigma^l} = 1 + \frac{1}{2\sigma^l} \int\limits_{h}^{\infty} \Pi(h)\,dh \tag{153}$$

Since $\cos\theta \leq 1$, the surface tension of the film must be less than the surface tension of the bulk solution, $\sigma^f < \sigma^l$, and the integral term in Eq. (153) must be negative in order for a nonzero contact angle to be formed. Hence, the contact angle, θ, and the transversal tension, τ (cf. Eq. 152), are integral effects of the long-range *attractive* surface forces acting in the transition zone between the film and Plateau border, where $h > h_1$ - see Fig. 17a.

In the case of a fluid particle attached to a surface (Fig. 18) the integral of the pressure $P_1(z) = P_1(z=0) - \Delta\rho g z$ over the particle surface equals the buoyancy force, F_b, which at equilibrium is counterbalanced by the disjoining pressure and transversal tension forces [253]

$$2\pi r_{c1} \tau = F_b + \pi r_{c1}^2 \Pi \tag{154}$$

F_b is negligible for bubbles of diameter smaller than c.a. 300 μm. Then the forces due to τ and Π counterbalance each other. Hence, at equilibrium the role of the repulsive disjoining pressure is to keep the film thickness uniform, whereas the role of the attractive transversal tension is to keep the bubble (droplet) attached to the surface. In other words, the particle sticks to the surface at the contact line where the long-range attraction prevails (see Fig. 17a), whereas the repulsion predominates inside the film, where $\Pi = P_c > 0$. Note that this conclusion is valid not only for particle-wall attachment, but also for particle-particle interaction. For zero contact angle τ is also zero (Eq. 152) and the particle will rebound from the surface (the other particle), unless some additional external force does keep it attached. The deeper understanding of such phenomena has not only fundamental, but also practical

importance for phenomena like flocculation in emulsions, or redeposition of oil droplets on solid surfaces in washing.
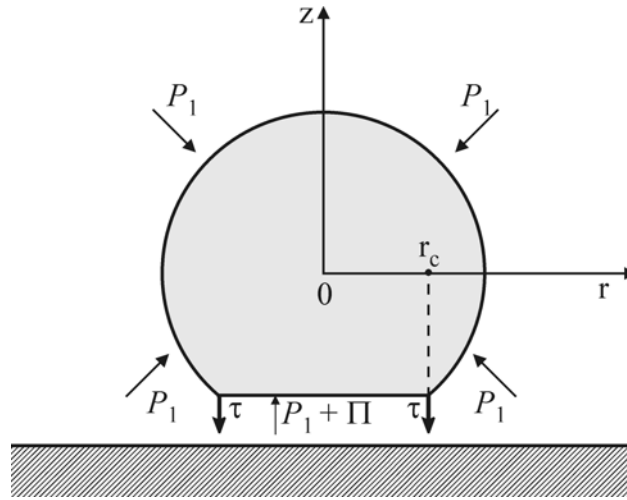

Fig. 18. Sketch of the forces exerted on a fluid particle (bubble, drop, vesicle) attached to a planar surface: Π is disjoining pressure, τ is transversal tension, P_1 is the pressure in the outer liquid phase.

B.2. Transition zone film - Plateau border

Macroscopic parameters like contact angle, θ, line and transversal tensions, κ and τ, can be deduced from the shape of the microscopic transition zone between the film and the Plateau border. From a microscopic viewpoint the transition between the film surface and the meniscus is smooth as depicted in Fig. 19 (the continuous lines). As the film thickness increases across the transition zone, the disjoining pressure decreases and tends to zero for h » 10 nm, cf. Fig. 17a and Fig. 19. Respectively, the surface tension varies from σ^f for the film to σ^l for the Plateau border. By using local force balance considerations one can derive the equations governing the shape of the meniscus in the transition zone; in the case of *axial symmetry*, depicted in Fig. 19, these equations read [252]

$$\frac{d}{dr}\left(\sigma \sin \varphi\right) + \frac{1}{r}\,\sigma(r)\sin \varphi(r) = P_c - \Pi(r) \tag{155}$$

$$-\frac{d}{dz}\left(\sigma \cos \varphi\right) + \frac{1}{r}\,\sigma(r)\sin \varphi(r) = P_c,\ \tan \varphi(r) = \frac{dz}{dr} \tag{156}$$

where $\varphi(r)$ is the running slope angle. Equations (155)-(156) allow calculation of the three unknown functions, $z(r)$, $\varphi(r)$ and $\sigma(r)$, provided that the disjoining pressure, $\Pi(r)$, is known from the microscopic theory. For example, $\Pi(r)$ may be approximately expressed through the

disjoining pressure $\Pi(h)$ of a plane-parallel film of thickness $h \equiv 2z(r)$, [254, 255]. By eliminating P_c between Eqs. (155) and (156) one can derive [252]

$$\frac{d\sigma}{dz} = -\Pi(r)\cos\varphi(r) \tag{157}$$

This result shows that the hydrostatic equilibrium in the transition region is ensured by simultaneous variation of σ and Π. Eq. (157) represents a generalization of Eq. (144) for a film of uneven thickness and axial symmetry. Generalization of Eqs. (155) - (156) for the case of more complicated geometry is also available [234].
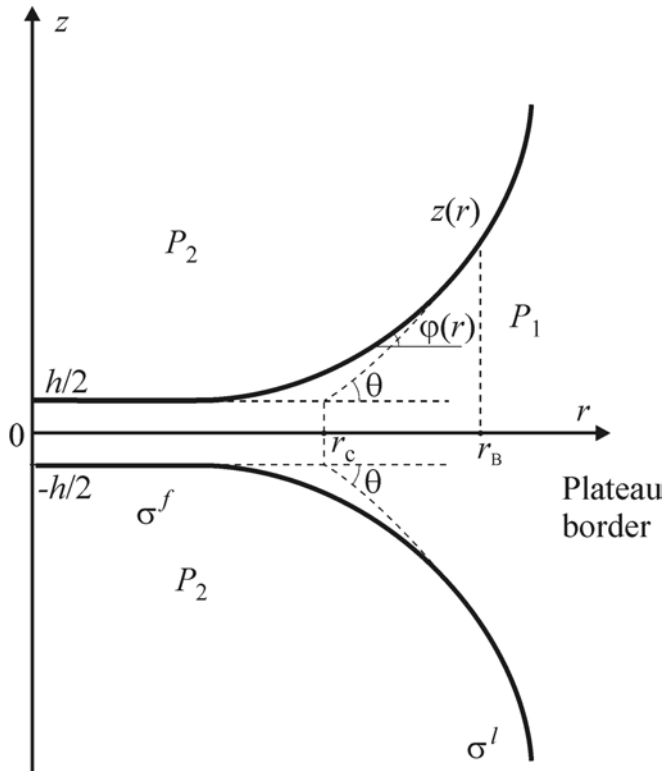

Fig. 19. Liquid film of thickness h: The solid lines represent the real interfaces, whereas the dashed lines show the extrapolated interfaces in the transition zone film - Plateau border; θ is the contact angle and $\varphi(r)$ is the running slope angle.

In the Plateau border $z \gg h$, $\Pi \to 0$, $\sigma \to \sigma^l$ = const and both Eqs. (155) and (156) reduce to the common Laplace equation of capillarity expressed in the following parametric form [256]:

$$\frac{d\sin\varphi}{dr} + \frac{\sin\varphi}{r} = P_c / \sigma^l \tag{158}$$

The macroscopic contact angle, θ, is defined as the angle at which the *extrapolated* meniscus, obeying Eq. (158), meets the *extrapolated* film surface [251] - see the dashed line in Fig. 19. The real surface, shown by solid line in Fig. 19, differs from this *extrapolated* (idealized) profile, because of the interactions between the two film surfaces, which is taken into account in Eq. (155), but not in Eq. (158). To compensate for the difference between the real and

idealized system, line and transversal tensions are ascribed to the contact line in the macroscopic approach. In particular, the line tension makes up for the differences in surface tension and running slope angle [252]

$$\frac{\widetilde{\kappa}}{r_c} = \int_0^{r_B} \left[\left(\frac{\sigma \sin^2 \varphi}{r \cos \varphi} \right)^{\text{real}} - \left(\frac{\sigma \sin^2 \varphi}{r \cos \varphi} \right)^{\text{idealized}} \right] dr; \qquad (159)$$

whereas τ compensates for the differences in surface forces (disjoining pressure):

$$\tau = \frac{1}{r_c} \int_0^{r_B} \left[(\Pi)^{\text{id}} - \Pi(r) \right] r \, dr \qquad (160)$$

where

$$(\Pi)^{\text{id}} = P_c \quad \text{for} \quad 0 < r < r_c;$$
$$(\Pi)^{\text{id}} = 0 \quad \text{for} \quad r > r_c.$$

The superscripts "real" and "idealized" in Eq. (159) mean that the quantities in the respective parentheses must be calculated for the real and idealized meniscus profiles; the latter coincide for $r > r_B$ - cf. Fig. 19.

Theoretical calculations based on the above micromechanical theory predict $\kappa \approx -10^{-12}$ N for foam films [257] and $\kappa \approx -10^{-13}$ N for emulsion films [258]. Correspondingly, the experiments [259] with foam films stabilized by sodium dodecyl sulfate (SDS) show that the *equilibrium* value of κ is zero in the framework of the experimental accuracy, $\pm 5 \times 10^{-9}$ N. Therefore it seems that the equilibrium line tension is a very small quantity and can be neglected in most cases (except may be in heterogeneous nucleation). On the other hand, comparatively large *non-equilibrium* values of the line tension, $\kappa \approx -10^{-7}$ N, have been measured with advancing menisci (shrinking bubbles). Such large values can be explained [260] by the strong short-range attraction between the two film surfaces in the case of secondary films stabilized by SDS [261-263]. The detachment of the two film surfaces in the process of meniscus advance is accompanied by significant local alterations of the interfacial shapes and tensions in the real dynamic transition zone, which contributes (cf. Eq. 159) to large values of the *dynamic* line tension. Moreover, if one carries out the same experiment, but with a *nonionic* surfactant, rather than with SDS, no detectable line tension is found out [264]. This is related to the absence of strong short-range attraction between the two nonionic surfactant adsorption monolayers, as indicated by the small contact angle which is not subjected to hysteresis in this case [264].

In conclusion, it should be noted that the width of the transition region between a thin liquid film and Plateau border is usually very small [257]- below 1 μm. That is the reason why the optical measurements of the meniscus profile give information about the thickness of the Plateau border in the region $r > r_B$ (Fig. 19). Then if the data are processed by means of Laplace equation, Eq. (158), one determines the contact angle, θ, as discussed above. In spite of being a purely macroscopic quantity, θ characterizes the magnitude of the surface forces inside the thin liquid film, as implied by Eq. (153). This has been first pointed out by Derjaguin [265] and Princen and Mason [266].

C. Contact Angle and Interaction between Surfactant Adsorption Monolayers

Equation (153) can be written in the form [245]

$$f = -2\sigma(1 - \cos\theta_0), \quad f \equiv \int_{h_0}^{\infty} \Pi(h)\,dh \tag{161}$$

where f is the free energy (per unit area) of interaction between the two film surfaces and $\sigma \equiv \sigma^I$. Indeed, the integral in Eq. (161) expresses the work for bringing the two film surfaces from infinity to a finite distance h_0. Therefore, the contact angle measurements provide a method for determining the interaction between two adsorption monolayers of amphiphilic molecules such as various surfactants, lipids, proteins. (See Ref. [267] for a review on the methods for thin film contact angle measurements.) In this aspect, the method based on measurement of contact angles is alternative and complementary to the surface force apparatus, which detects the force between two crossed mica cylinders [4]. The advantage of the contact angle measurements is that the experimental system is relatively simple, self-adjusting, inexpensive, and allows measurements with fluid interfaces. A drawback of the method is that it allows measurements only in a restricted range(s) of film thicknesses, corresponding to $\partial\Pi/\partial h < 0$, see e.g. Ref. [268].

C.1. Hysteresis of the contact angle

In the case when the equilibrium film is *secondary* ($h = h_2$ in Fig. 17a), hysteresis of the contact angle is often observed. This allows one to measure three experimental parameters (instead of one): the *equilibrium* contact angle, θ_0, the *advancing* contact angle, θ_A, and the

receding contact angle, θ_R. In particular, θ_A corresponds to *detachment* of the two film surfaces, while θ_R corresponds to *attachment* of the film surfaces. For example, the following values have been measured [269] with foam films stabilized by the protein lyzozyme at pH = 11.5: $\theta_R = 2.3^o$, $\theta_0 = 3.2^o$, $\theta_A = 16.4^o$. Contact angle hysteresis has been observed also with foam films stabilized with sodium dodecyl sulfate [270]. These are examples for contact angle hysteresis observed with molecularly smooth and homogeneous surfaces; in this case the hysteresis is due to the action of the surface forces in the film [271].

In general, $\theta_R \leq \theta_0 \leq \theta_A$. The difference between the contact angle hysteresis with liquid films and with solid surfaces is that in the former case an equilibrium angle does exist, whereas in the latter case there is no specified equilibrium contact angle in the range between θ_R and θ_A. For equilibrium *primary* liquid films ($h = h_1$ in Fig. 17a) the values of the three angles usually coincide in the framework of the experimental accuracy.

In principle, the experimental data about θ_R, θ_0, and θ_A allow one to extract information about the shape of the $\Pi(h)$-isotherm, cf. Fig. 17a, by using an appropriate model $\Pi(h)$-curve depending on several parameters, which are to be determined from the comparison with the experiment, see e.g. Ref. [254, 255]. The measured value of θ_0 can be interpreted by means of Eq. (161), were h_0 is the equilibrium thickness of the film. The values of θ_A and θ_R can be interpreted on the basis of the theory by Martynov *et al.* [271, 272], which is briefly outlined below.

Let us consider a planar thin liquid film in contact with a Plateau border. The capillary pressure $P_c = P_2 - P_1$ can be varied by ejection or injection of liquid through the orifice in the wall of the Scheludko cell [273], see Fig. 20. Such a process is accompanied by receding or advance of the capillary meniscus.

For the sake of simplicity we consider a Plateau border of translational symmetry along the *y*-axis, Fig. 20. In addition, we assume that the vertical wall is well wettable by the liquid, i.e. $dz/dx \rightarrow \infty$ at the wall. The last two assumptions do not restrict the validity of the final expressions for θ_R, θ_0, and θ_A in so far as the dependence of the contact angle on the capillary pressure and the curvature of the contact line is negligible.
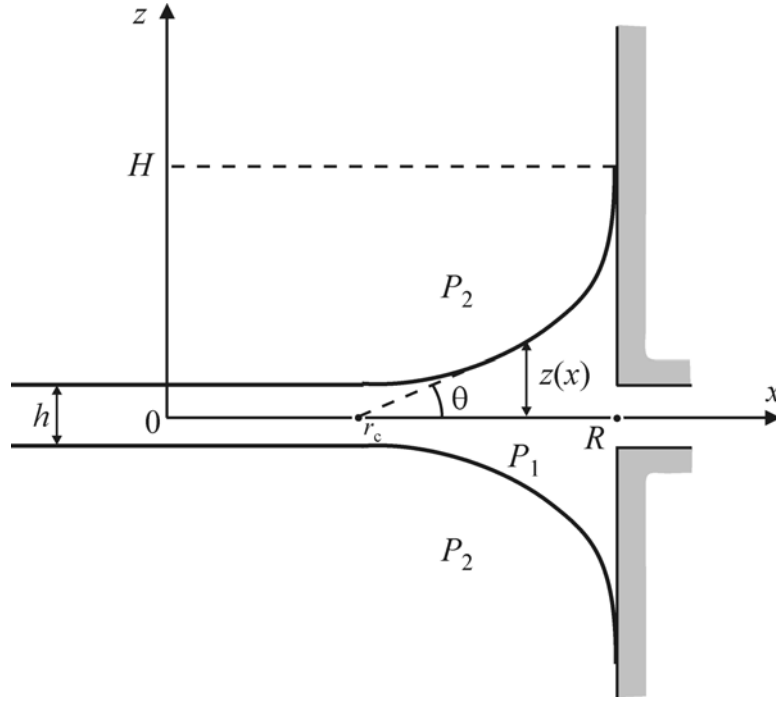
Fig. 20. Sketch of the transition zone film - Plateau border in a Scheludko cell; h is the film thickness, θ is the contact angle subtended between the extrapolated meniscus (the dashed line) and the film midplane.

The meniscus profile *z(x)* obeys a counterpart of Eq. (155):

$$\frac{\sigma z''}{\left(1+z'^2\right)^{3/2}}=P_c-\Pi(h) \tag{162}$$

where the prime denotes *d/dx*, and $h = 2z(x)$. The variation of σ along the transition zone is small ($\Delta\sigma/\sigma < 1\%$) and is neglected in the present derivation. The extrapolated meniscus profile, $\tilde{z}\,(x)$, (the dashed line in Fig. 20) obeys a counterpart of Eq. (158),

$$\frac{\sigma\tilde{z}''}{\left(1+\tilde{z}'^2\right)^{3/2}}=P_c \tag{163}$$

which follows from Eq. (162) for $\Pi = 0$. The respective boundary conditions are

$$\tilde{z}'\,(r_c)=\tan\theta; \qquad z(R)=\tilde{z}(R)=H; \qquad z'(R)=\tilde{z}'(R)=\infty \tag{164}$$

- see Fig. 20. Multiplying Eq. (163) by $\tilde{z}'$ and integrating form $\tilde{z}=0$ to $\tilde{z}=H$ one obtains

$$HP_c=\sigma\cos\theta \tag{165}$$

A similar integration of Eq. (162) from $z = h/2$ to $z = H$ yields [271, 272]

$$\frac{2\sigma}{\sqrt{1+z'^2}} = \psi(h,P_c) \tag{166}$$

where

$$\psi(h, P_c) \equiv (2H - h)P_c - \int_h^\infty \Pi(h)dh \tag{167}$$

At equilibrium the meniscus surface levels off at the planar film surface, where $z' = 0$. Setting $z' = 0$ in Eq. (166), in keeping with Eq. (167) one obtains

$$2\sigma = 2HP_0\left(1 - \frac{h_0}{2H}\right) - \int_{h_0}^\infty \Pi(h)dh \tag{168}$$

where P_0 and h_0 are the values of P_c and h corresponding to the equilibrium state. Neglecting the term $h_0/2H$ in the parenthesis and substituting HP_0 from Eq. (165) one arrives at the expression for the equilibrium contact angle,

$$\cos\theta_0 = 1 + \frac{1}{2\sigma}\int_{h_0}^\infty \Pi(h)dh \tag{169}$$

cf. Eq. (153). The differentiation of Eq. (167) yields

$$\frac{\partial\psi}{\partial h} = \Pi - P_c \tag{170}$$

The comparison of the last equation with Eq. (135) shows that the dependence ψ vs. h has extrema in the points $h = h_1, h_2, h_3$, see Fig. 17b. Moreover, for the equilibrium film one has $\psi = 2\sigma$ (set $z' = 0$ in Eq. 166) - see the horizontal dashed line in Fig. 17b, corresponding to the stable secondary film with $h = h_2$.

C.2. Expression for the advancing contact angle

Fig. 21 represents a close vicinity of the contact zone film - Plateau border; the small rectangles symbolize the amphiphilic molecules of the two adsorption monolayers. The peripheral molecules of the film experience a normal force per unit length, $\sigma\sin\theta_{cr}$, which tends to detach the two film surfaces. In fact, θ_{cr} denotes the critical value of the *microscopic* contact angle corresponding to the onset of detachment of the peripheral molecules and the beginning of the meniscus advance. The respective values of the capillary pressure are $P_c = P_A$ and $h = h_A$. The angle θ_{cr} is to be distinguished from the *macroscopic* advancing contact angle, θ_A, which is related to the slope of the *extrapolated* meniscus surface at the film midplane, see Fig. 21.

Applying Eqs.(165)-(167), with $z'(r_c) = \tan\theta_{cr}$, to the advancing meniscus one derives

$$H_A P_A = \sigma\cos\theta_A \tag{171}$$

$$2\sigma\cos\theta_{cr} = 2H_A P_A \left(1 - h_A/2H_A\right) - \int_{h_A}^\infty \Pi(h)dh \tag{172}$$
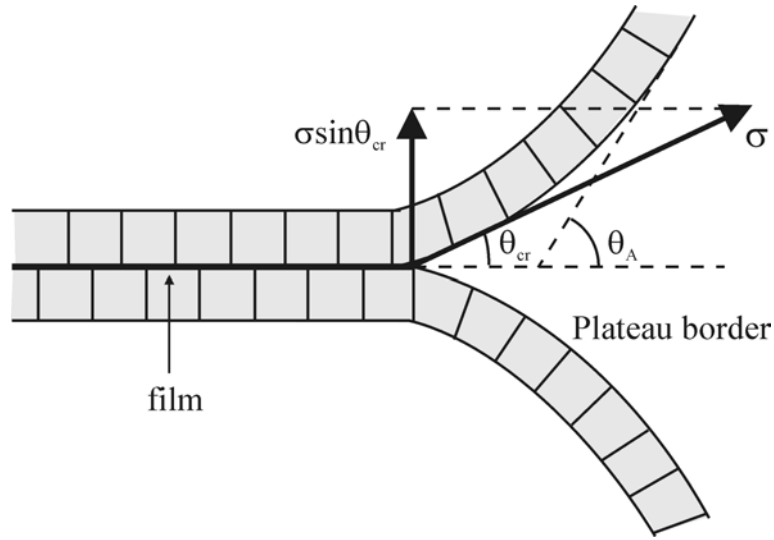
Fig. 21. Sketch of a secondary film representing two attached monolayers of amphiphile molecules (the rectangles); $\sigma\sin\theta_{cr}$ is the critical force per unit length of the film periphery causing detachment of the peripheral molecules.

Neglecting the second term in the parenthesis and combining Eqs. (171) and (172) one obtains an expression for the advancing contact angle:

$$\cos\theta_A = \cos\theta_{cr} + \frac{1}{2\sigma}\int_{h_A}^{\infty}\Pi(h)dh \tag{173}$$

The expression proposed by Martynov *et al.* [271] corresponds to setting $\theta_{cr} = \pi/2$ in Eq. (173). The first term in the right-hand side of Eq. (173) expresses the contribution of the contact adhesion, whereas the integral term expresses the contribution of the long-range interaction. Comparing Eqs. (169) and (173) one obtains

$$\cos\theta_0 - \cos\theta_A = 1 - \cos\theta_{cr} + \frac{1}{2\sigma}\int_{h_0}^{h_A}\Pi(h)dh \tag{174}$$

As the $\Pi(h)$-isotherm is rather steep for secondary films, one may expect that $h_A \approx h_0$ and the integral term in Eq. (174) can be neglected. If such is the case, it turns out that the difference between the equilibrium and the advancing contact angles is determined entirely by $\cos\theta_{cr}$, i.e. by the contact adhesion.

The depth of the primary minimum, Π_{min}, may be estimated from the value of the advancing contact angle as follows. Since Π is force per unit area, then Πa (with a being area per adsorbed amphiphile molecule) gives force per molecule. Then the critical force, f_{cr}, needed to detach two adhered amphiphile molecules can be identified with

$$f_{cr} = |\Pi_{min}| a \tag{175}$$

On the other hand, from Fig. 21 one realizes that $f_{cr} = \sigma\sqrt{a}\sin\theta_{cr}$. Then in view of Eq. (175) one obtains

$$|\Pi_{min}| = \frac{\sigma}{\sqrt{a}}\sin\theta_{cr} \tag{176}$$

With the aforementioned values measured with lysozyme, $\theta_0 = 3.2^o$, $\theta_A = 16.4^o$, $\sqrt{a}$=3.4 nm and by means of Eqs. (174) and (176) one estimates θ_{cr}=16.08^o and $\Pi_{min} = -4.4\times10^7$ dyn/cm^2.

One may define $w_{cr} = 2\sigma(1 - \cos\theta_{cr})$ as the critical work of detachment of the two adsorption monolayers. With the above value of θ_{cr} and $\sigma = 54$ dyn/cm one calculates $w_{cr} = 2.1$ erg/cm^2 for two attached lysozyme monolayers.

C.3. Expression for the receding contact angle

Imagine an equilibrium initial state of the film, corresponding to $P_c = P_0$, $h = h_2$ and $\psi = 2\sigma$, see Fig. 17b. Even an infinitesimal increase of P_c will break the equilibrium condition $\psi = 2\sigma$, cf. Eq. (167), and the ψ vs. h curve will move upwards (see the dotted line in Fig 17b). This will cause a motion (receding) of the meniscus, accompanied by attachment of the two meniscus surfaces [271]. From Eq. (166), transformed to read

$$z' = [(2\sigma/\psi)^2 - 1]^{1/2}, \tag{177}$$

one sees that the domain of film thicknesses, for which $\psi > 2\sigma$, is unstable, because z' in Eq. (177) takes imaginary values. More precisely, the viscous forces, not accounted for in Eq. (177), affect the meniscus shape in this narrow region.

At some $P_c = P_R$ the maximum at $h = h_1$ (see the dotted line in Fig. 17b) will touch the line $\psi = 2\sigma$. Then for any $P_c > P_R$ the region around $h = h_1$ becomes also unstable. Thus the meniscus motion responses much more easily to the applied increased capillary pressure. As pointed out by Martynov *et al.* [271], the receding of the meniscus takes place at the critical conditions, $P_c = P_R$ and $\theta = \theta_R$, with θ_R being the receding contact angle. As shown in Fig 17b, the maximum of the dotted $\psi(h)$ curve, which touches the line $\psi = 2\sigma$, corresponds to a metastable primary film. From a physical viewpoint this means that a thicker primary film

will be left after the receding contact line. In fact, this is what is observed experimentally: a narrow belt of greater thickness is present in an intermediate vicinity behind the receding meniscus [269, 274, 275]. Applying Eqs.(165)-(167) to the receding meniscus ($H = H_R$, $P_c = P_R$) one derives [271]

$$H_R P_R = \sigma \cos \theta_R \tag{178}$$

$$2\sigma = 2H_R P_R \left(1 - h_R / 2H_R\right) - \int_{h_R}^{\infty} \Pi(h) dh \tag{179}$$

where h_R denotes the thickness of the film (corresponding to the maximum of the dotted line with $\psi = 2\sigma$ in Fig. 17b) left after the receding Plateau border. Neglecting the second term in the parenthesis in Eq. (179), and combining it with Eq. (178), one obtains an expression for the receding contact angle:

$$\cos \theta_R = 1 + \frac{1}{2\sigma} \int_{h_R}^{\infty} \Pi(h) dh \tag{180}$$

The comparison between Eqs. (169) and (180) yields

$$\cos \theta_0 - \cos \theta_R = \frac{1}{2\sigma} \int_{h_0}^{h_R} \Pi(h) dh \tag{181}$$

For $\Pi(h)$ isotherms like that depicted in Fig. 17a the integral in the right-hand side of Eq. (181) is typically negative; this implies that $\theta_0 > \theta_R$, which is the usual experimental situation. Eq. (181) shows that θ_R brings information about the shape of the $\Pi(h)$-isotherm in the region of the loop ($h_2 < h < h_R \approx h_1$), cf. Fig. 17a. One can extract this information by using an appropriate model $\Pi(h)$-curve depending on several parameters, which are to be determined from the comparison with the experiment.

D. Films of Uneven Thickness

The gap between two colliding particles (bubbles, droplets, solid particles, surfactant micelles) in a colloidal dispersion can be treated as a film of uneven thickness. Then it is possible to utilize the theory of thin films to calculate the energy of interaction between two colloidal particles. Derjaguin [276] has derived an approximate formula, which expresses the energy of interaction between two *spherical* particles of radii R_1 and R_2 through integral of the excess surface free energy per unit area, $f(h)$, of a plane-parallel film of thickness h (see Eq. (161) above):

$$U(h_0) = \frac{2\pi R_1 R_2}{R_1 + R_2} \int_{h_0}^{\infty} f(h)\, dh \qquad (182)$$

Here h_0 is the shortest distance between the surfaces of the two particles and $U(h_0)$ is the respective particle-particle interaction energy, see Fig. 22. In the derivation of Eq. (182) it is assumed that the interaction between two parcels from the particle surfaces, separated at the distance h, is approximately the same as that between two similar parcels in a plane-parallel film. This assumption is correct when the range of action of the surface forces and the distance h_0 are small compared to the curvature radii R_1 and R_2. It has been established, both experimentally [4] and theoretically [277], that Eq. (182) provides a good approximation in the range of its validity.
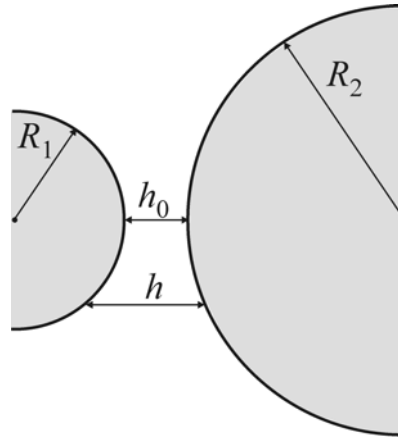

Fig. 22. Two spherical particles of radii R_1 and R_2; h_0 and h are the shortest and the running surface-to-surface distance, respectively.

Eq. (182) can be generalized for smooth surfaces of arbitrary shape (not necessarily spheres). For that purpose the surfaces of the two particles are approximated with paraboloids in the vicinity of the point of closest approach ($h = h_0$). Let the principal curvatures at this point be c_1 and c_1' for the first particle and c_2 and c_2' for the second particle. Then the generalization of Eq. (182) reads [2]

$$U(h_0) = \frac{2\pi}{\sqrt{C}} \int_{h_0}^{\infty} f(h)\, dh, \qquad (183)$$

$$C \equiv c_1 c_1' + c_2 c_2' + \left(c_1 c_2 + c_1' c_2' \right) \sin^2 \omega + \left(c_1 c_2' + c_1' c_2 \right) \cos^2 \omega$$

where ω is the angle subtended between the directions of the principle curvatures of the two approaching surfaces. For two spheres one has $c_1 = c_1{}' = 1/R_1$, $c_2 = c_2{}' = 1/R_2$ and Eq. (183) reduces to Eq. (182).

For two cylinders of radii r_1 and r_2 crossed at angle ω one has $c_1 = c_2 = 0$; $c_1{}' = 1/r_1$, $c_2{}' = 1/r_2$ and Eq. (182) yields

$$U\left(h_0\right) = \frac{2\,\pi\,\sqrt{r_1\,r_2}}{\sin\omega} \int_{h_0}^{\infty} f\left(h\right) dh \qquad (184)$$

Eq. (184) is often used in connection to the experiments with the surface force apparatus [4, 278], where the surfaces represent two crossed cylindrical mica sheets. The divergence in Eq. (184) for $\omega = 0$ is related to the fact that the axes of the two infinitely long cylinders are parallel for $\omega = 0$ and thus the area of the zone of interaction becomes infinite. Eq. (184) can be also utilized to calculate the energy of interaction between two cylindrical surfactant micelles.

The Derjaguin approximation is applicable to any type of force law (attractive, repulsive, oscillatory) if the range of the forces is much smaller than the particles radii. It reduces the problem for interactions between particles to the simpler problem for interactions in plane-parallel films, which are reviewed in the next section.

Part 2 of this review and the List of References can be found at:
http://www.lcpe.uni-sofia.bg/publications/1999/pdf/1999-10-2-KD-PK-II.pdf